ENTRAINMENT PHENOMENON IN STRATIFIED LIQUID LAYERS BY IMPOSING ROTARY MOTION

Thesis submitted in partial fulfillment of the requirement for the degree of

Master of Technology

In

Mechanical Engineering

By

Jishnu M (Roll Number: 213ME3436)

Under the guidance of

Dr. Suman Ghosh

DEPARTMENT OF MECHANICAL ENGINEERING
NATIONAL INSTITUTE OF TECHNOLOGY ROURKELA
ROURKELA-769008

JUNE-2015

CERTIFICATE

*This is to certify that the thesis entitled "**Entrainment Phenomenon in Stratified Liquid Layers by Imposing Rotary Motion**", submitted by **Jishnu M (Roll Number: 213ME3436)** to National Institute of Technology, Rourkela, is a record of bona fide research work under my supervision, to the best of my knowledge in partial fulfilment of the requirements for the degree of **Master of Technology** in the Department of Mechanical Engineering, National Institute of Technology Rourkela.*

Place: Rourkela
Date:

Dr. Suman Ghosh
Assistant Professor
Department of Mechanical Engineering
National Institute of Technology Rourkela
Rourkela-769008, Odisha, India.

DECLARATION

I certify that

a. The work contained in the thesis is original and has been done by myself under the general supervision of my supervisor(s).
b. The work has not been submitted to any other Institute for any degree or diploma.
c. I have followed the guidelines provided by the Institute in writing the thesis.
d. I have conformed to the norms and guidelines given in the Ethical Code of Conduct of the Institute.
e. Whenever I have used materials (data, theoretical analysis, and text) from other sources, I have given due credit to them by citing them in the text of the thesis and giving their details in the references.
f. Whenever I have quoted written materials from other sources, I have put them under quotation marks and given due credit to the sources by citing them and giving required details in the references.

Date: Jishnu M (Roll Number: 213ME3436)
Place: Signature of the Student

Curriculum Vita

Name : **JISHNU.M**

Address : MANIMANGALATHU HOUSE

PUTHENCAVU P O

ANGADICAL, CHENGANNUR

ALAPPUZHA - 689123

Phone. No : 7736719480, 7750826265, 04792456405

Email id : jishnurit@yahoo.com, jishnurit@gmail.com.

Educational qualification:

Class X : He has passed Xth from St Gregorious Senior secondary school, Mulakuzha, Chengannur in the year 2006.

Class XII: He has passed XIIth from St Gregorious Senior secondary school, Mulakuzha, Chengannur in the year 2008.

B Tech : He has passed B tech from Govt. Rajiv Gandhi Institute of Technology, Kottayam in the year 2012.

ACKNOWLEDGEMENT

It is always a pleasure to acknowledge with gratitude the help received from various sources and persons. First and foremost I thank GOD Almighty for the blessings showered upon me during the project works.

I wish to extend my thanks to my project guide **Dr. Suman Ghosh** (Assistant Professor, Department of Mechanical Engineering) for his support and inspiring guidance towards the progress of my project.

I want to express my gratitude to **Dr. Siba Sankar Mohapatra**, Head of Department Mechanical Engineering, for his support. I would like to thank **Prof. A.K. SATAPATHY** of the mechanical engineering department for providing the CFD lab where I have done the major part of my project work.

I would also thank all the faculty members of the Mechanical Engineering Department, NIT Rourkela for their guidance and kind co-operation. I also thank my parents and friends who stood by me giving enough encouragement and support in the successful completion of this project work.

Date: Jishnu M (213ME3436)

Place:

CONTENTS

LIST OF TABLE

LIST OF FIGURES

LIST OF ABBREVIATIONS & SYMBOLS

Abbreviations	
d	Diameter of the rotor, m.
h	Distance between the interface and rotor top, m.
ω	Rotational speed of rotor, rad/s.
rad/s	Radians per second.
VF	Volume Fraction.
FVM	Finite Volume Method.

Symbols	
u	Magnitude of velocity along x-direction, m/s
v	Magnitude of velocity along y-direction, m/s
P	Pressure force, N/m^2
k	Turbulent kinetic energy
S	User-defined source terms
ρ	Density, kg/m^3
μ	Dynamic viscosity, $N-s/m^2$
∇	Differential operator
ε	Turbulent dissipation rate

ABSTRACT

An attempt is made to study the entrainment phenomena in a stratified liquid layers by imposing rotary motion using numerical simulation as well as experimental investigation. The different cases are studied by placing a rotor at different locations either in the heavier fluid or in the interfaces. The phenomena is also studied by varying the rotor diameter and rotor speed used. Phase contours at different time instants are produced for each of the cases. The rate at which one phase is entering in to the other is also studied for each of the cases. Comparisons between the rates of entrainment with different cases are also made. The phase contour obtained through experimental observation are also presented at a regular interval of time.

Keywords: Entrainment, Multiphase flow, Volume fraction, Finite Volume Method (FVM), Volume of Fluid (VOF), Rotary motion, Stratified layer.

CHAPTER 1:

INTRODUCTION & LITERATURE SURVEY

This chapter contains an introduction to the phenomenon of entrainment in startified liquid layers in multiphase flow, an extensive literature survey, gaps in the literatures, aims and objectives of the present works, and organization of the thesis.

1.1 INTRODUCTION

Entrainment is the phenomenon of transport of fluid molecules across an interface between two fluid layers by a shear induced turbulent flux. Entrainment is observed in the systems in which the two phases are in relative motion. Stratified flow is defined as the flow of immiscible fluids which are separated by a clear and distinguishable interface.

The study of entrainment phenomena is of great importance in designing the mixing chambers of chemical reactors. Another important application of entrainment phenomena is in paint and pharmaceutical companies where the different chemical reactants are to be mixed in different proportions.

The atmospheric layers acts like stratified liquid layers and the entrainment occurring at different interfaces of this layers affects the climate. The entrainment study can be of great help in understanding the physics behind this mixing and is of great importance for climate studies.

1.2 LITERATURE SURVEY

Wolanski et al. (1974) studied experimentally and theoretically the turbulent entrainment occurring at the interface of stable density stratified structures. The buoyancy flux was observed to be functions of richardson number and prandtl number. Wilkinson et al. (1975) studied the air entrainment in to a liquid by a cylindrical rotor which was previously no wetted. Narimousa et al. (1985) studied the entrainment occurring as a result of turbulent shear flow at the interface of a stably stratified fluid.

The lower most layer is non turbulent layer and upper most layer is turbulent, the flow is induced in a recirculating channel with the help of a disc pump. Alanson et al. (1990) studied the entrainment of heavier fluid by a lighter fluid which is moving upward from the bottom to the top layer. Thoroddsen et al. (1997) experimentally studied the coating flows occurring in a partially filled rotating cylinder which is rotating about its horizontal axis. Xiaoliang et al (2012) studied experimentally the air entrainment by a plunging jet at the surface of a liquid and the jet penetration depth was determined. Roy et al. (2013) studied the air entrained in to the water surface by a jet of water striking the surface of the water and taking the images during the event to study the depth up to which the air was entrained in to the water surface. Zhaoming et al. (2014) studied the entrainment phenomena through small-scaled ADS-4 in AP1000 both experimentally and theoretically. Kulkarni et al. (2014) carried out the CFD modelling to study the gas entrainment in stirred tank systems. Two types of impellers were used for studying and the onset of the entrainment was predicted in terms of interfacial turbulence

1.3 GAPS IN LITERATURE

Entrainment phenomenon involving air and different liquids were studied earlier. But, the study on entrainment in stratified layers for two different liquids by the rotary motion of a rotor has not been found much according to the best of the authors' knowledge.

1.4 AIMS AND OBJECTIVES

An attempt has been made to study the entrainment of one liquid in to the other due to the rotary motion imposed in a stratified liquid layer. Here the basic objective is to study

the pattern and rate of entrainment and to calculate the volume fraction of the entrained phase by considering

1. Variation of the rotor diameter.
2. Variation of the rotor speed.
3. Variation of the position of the rotor.
4. Variation of the liquid pair used.

1.5 ORGANIZATION OF THE THESIS

The chapter 2 describes the problems considering different cases. The experimental setup is also described in chapter 2. In chapter 3, the methodology adopted to solve the problem is described. It includes the governing equations used, the grid pattern employed, the boundary conditions imposed, the parameters used for simulation and the convergence criteria set. The chapter 4 describes the results obtained and the corresponding discussions in details. Chapter 5 contains the concluding remarks obtained from the results and the possibilities for future works related to the present work.

Chapter 2:

PROBLEM FORMULATION

A cubic container contains two liquids which are immiscible to each other. These liquids will form a stratified liquid layer in the tank where the heavier liquid will occupy the bottom half and the lighter liquid will occupy the upper half. Two cases are considered, where in the first case, the rotor centre coincides with the interface of two fluids and in the second case the rotor is placed below the interface. The entrainment pattern and the volume fraction of the one phase entrained in to the other will be calculated for different cases by varying the rotor diameter (d), the rotor speed (ω), the distance between rotor top and interface (h) and also the liquid pair..

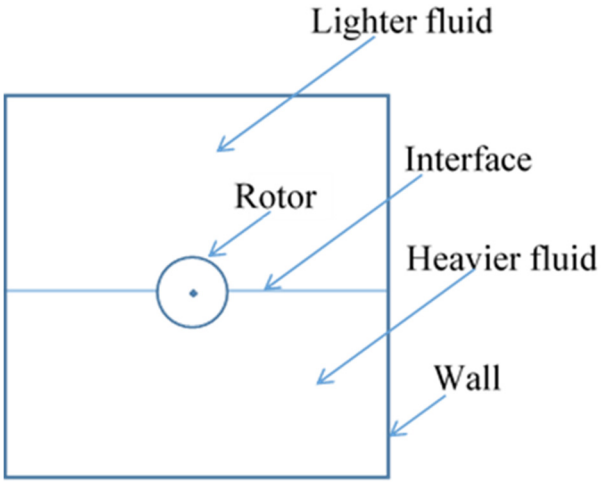

Figure 2.1: The rotor Centre coinciding with the interface of the two fluids

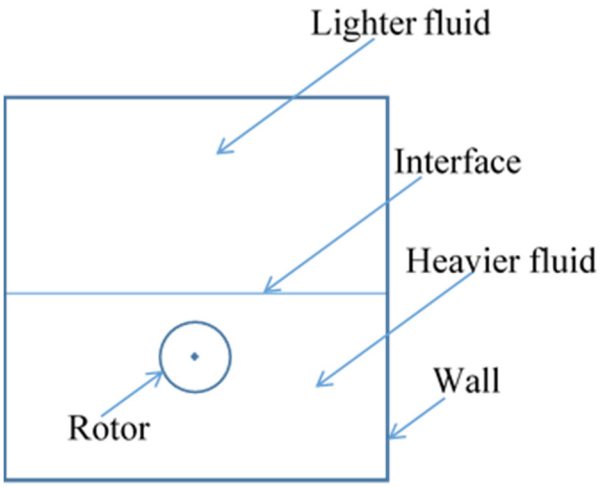

Figure 2.2: The rotor lying below the interface of the two fluids

2.1 THROUGH NUMERICAL SIMULATION

The following 16 cases were considered for studying the phenomenon of entrainment occurring at the interface of stratified liquid layers through numerical simulation. The cases were considered by varying diameter of the rotor (d), the angular speed of the rotor (ω), distance between rotor top and interface (h) and the fluid pair used. The dimensions of the tank (1m × 1m) and the level of the two liquids (0.5 m for each) in the tank were kept constant.

The different cases under consideration for numerical study.

2.1.1: h = 0.05 m, d = 0.1m, ω = 10 rad/s. Fluid pair = Water-Diesel.

2.1.2: h = 0.1 m, d = 0.2 m, ω = 10 rad/s. Fluid pair = Water-Diesel.

2.1.3: h = 0.05 m, d = 0.2 m, ω = 10 rad/s. Fluid pair = Water-Diesel.

2.1.4: h = 0.05 m, d = 0.2 m, ω = 20 rad/s. Fluid pair = Water-Diesel.

2.1.5: h = 0.025 m, d = 0.2 m, ω = 20 rad/s. Fluid pair = Water-Diesel.

2.1.6: h = 0.2 m, d = 0.4 m, ω = 10 rad/s. Fluid pair = Water-Diesel.

2.1.7: h = 0.05 m, d = 0.1 m, ω = 100 rad/s. Fluid pair = Water-Diesel.

2.1.8: h = 0.1 m, d = 0.2 m, ω = 50 rad/s. Fluid pair = Water-Diesel.

2.1.9: h = 0.015 m, d = 0.2 m, ω = 200 rad/s. Fluid pair = Water-Diesel.

2.1.10: h = 0.025 m, d = 0.2 m, ω = 50 rad/s. Fluid pair = Water-Diesel

2.1.11: h = 0.025m, d = 0.2 m, ω = 100 rad/s. Fluid pair = Water-Diesel.

2.1.12: h = 0.025 m, d = 0.2 m, ω = 200 rad/s. Fluid pair = Water-Diesel.

2.1.13: h = 0.05 m, d = 0.2 m, ω = 50 rad/s. Fluid pair = Water-Diesel.

2.1.14: h = 0.05 m, d = 0.2 m, ω = 100 rad/s. Fluid pair = Water-Diesel.

2.1.15: h = 0.05 m, d = 0.2 m, ω = 200 rad/s. Fluid pair = Water-Diesel.

2.1.16: h = 0.025 m, d = 0.2 m, ω = 200 rad/s. Fluid pair = Water-Engine oil.

2.2 THROUGH EXPERIMENT

An experiment is performed in a 12 cm × 12 cm cubical tank made by perspex sheet of 6 mm width. The rotor material used was PVC and a micro motor was used for providing rotational speed of the rotor. The voltage supplied to the micro motor was varied with the help of an elemeter to attain two different speeds. The fluid pair used for carrying out the experiment was water-kerosene and the whole phenomenon was recorded with the help of a camera.

CHAPTER 3:

METHODOLOGY

3.1 NUMERICAL CALCULATIONS

The 2D Finite Volume Method (FVM) with Volume of Fluid (VOF) multiphase model has been used for the present simulation. The VOF surface tracking technique with pressure-based solver in 2D version has been used to simulate the complex interface. The Pressure-based Implicit Splitting of Operators (PISO) method has been used. For turbulent modelling k-ε turbulent model is used.

3.2 GEOMETRY

The geometry is generated in work bench software. At first a square of 1m × 1m is drawn and then a circle is drawn inside that square, then the sketch is converted into a surface by using the surface from sketches option.

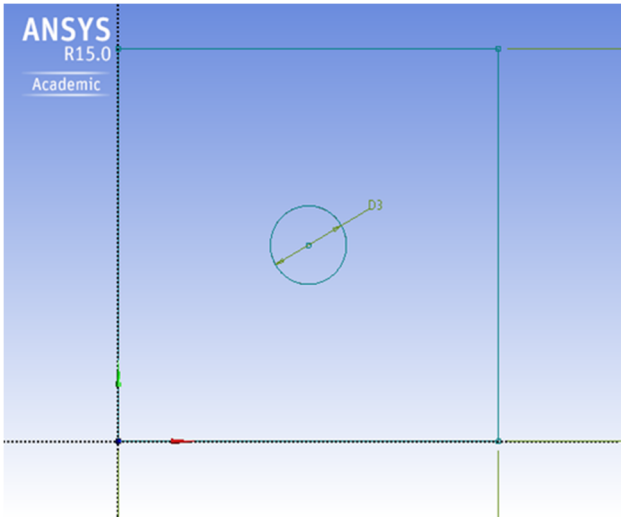

Figure 3.1: Geometry created using workbench

3.3 GRID PATTERN

After an extensive verification, the triangular elements have been considered for meshing the geometrical model. Grid size of 0.01 m has been chosen through an extensive grid independence test.

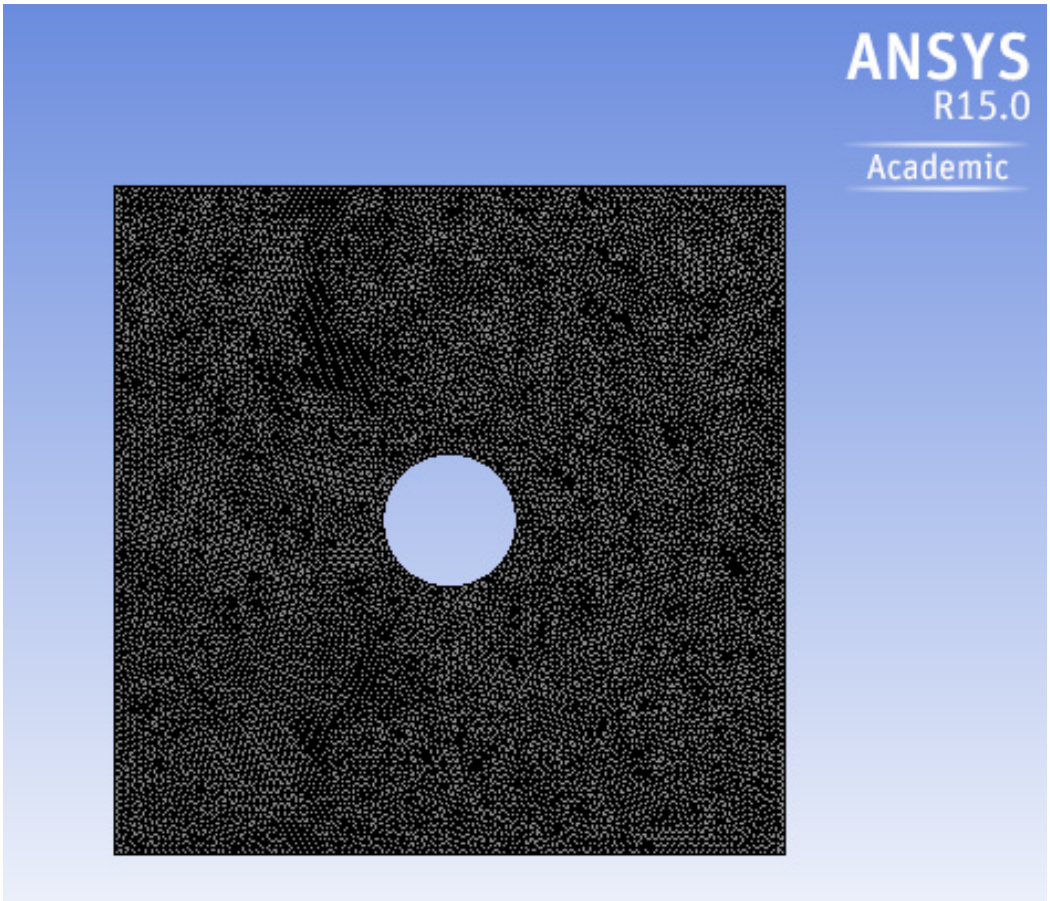

Figure 3.2: Mesh pattern employed for the present problem.

3.4 GOVERNING EQUATIONS

3.4.1 Continuity Equation

$$\frac{\partial}{\partial t}\left(\alpha_q \rho_q\right)+\nabla.\left(\alpha_q \rho_q \vec{v}_q\right)=\sum_{p=1}^{n}(\dot{m}_{pq}-\dot{m}_{qp})+S_q \tag{3.1}$$

3.4.2 Momentum Equation (N-S equation)

$$\frac{\partial}{\partial t}\left(\alpha_q \rho_q \vec{v}_q\right)+\nabla.\left(\alpha_q \rho_q \vec{v}_q \vec{v}_q\right)=-\alpha_q \nabla p+\nabla.\bar{\bar{\tau}}_q+\alpha_q \rho_q \vec{g}$$
$$+\sum_{p=1}^{n}\left(\vec{R}_{pq}+\dot{m}_{pq}\vec{v}_{pq}-\dot{m}_{qp}\vec{v}_{pq}\right)+ \tag{3.2}$$
$$\left(\vec{F}_q+\vec{F}_{lift,q}+\vec{F}_{wl,q}+\vec{F}_{vm,q}+\vec{F}_{vm,q}+\vec{F}_{td,q}\right)$$

3.4.3 Turbulence Modelling

$$\frac{\partial}{\partial t}(\rho k)+\frac{\partial}{\partial x_i}(\rho k u_i)=\frac{\partial}{\partial x_j}\left[\left(\mu+\frac{\mu_t}{\sigma_k}\right)\frac{\partial k}{\partial x_j}\right]+G_k+G_b-\rho\varepsilon-Y_M+S_k \quad (3.3)$$

$$\frac{\partial}{\partial t}(\rho \varepsilon)+\frac{\partial}{\partial x_i}(\rho \varepsilon u_i)=\frac{\partial}{\partial x_j}\left[\left(\mu+\frac{\mu_t}{\sigma_i}\right)\frac{\partial \varepsilon}{\partial x_j}\right]+C_{1i}\frac{\varepsilon}{k}(G_k+C_3G_b)-C_{2i}\rho\varepsilon 2k+Se \quad (3.4)$$

Where μ_t is called as turbulent viscous coefficient and is given as $\mu_t=\rho C_\mu \frac{k^2}{\varepsilon}$ (3.5)

3.4.4 Volume Fraction Equation

$$v_q=\int \alpha_q dv \quad (3.6)$$

$$\sum_{q=1}^{n}\alpha_q=1 \quad (3.7)$$

3.5 VALUES OF THE PARAMETERS FOR SIMULATION

Values of the constants in the governing equations are given in Table 3.1. Turbulence parameters were set as, turbulent kinetic energy (k) = 0.0225 m^2/s^2, turbulent dissipation rate (ε) = 0.00792 $m2/s^3$. The fluid properties were set as, interfacial tension for water-diesel pair = 0.028 N/m water-engine oil pair = 0.0092 N/m, density of water = 998.2 kg/m^3, water-viscosity = 0.001003 Pa-s. Density of diesel = 730 kg/m^3, diesel-viscosity = 0.0024 Pa-s. Density of engine oil = 884 kg/m^3, engine oil-viscosity = 0.486 Pa-s.

Table 3.1: Values of the model constants in the governing equations.

Values of the model constants				
$C_{1\varepsilon}$	$C_{2\varepsilon}$	$C_{3\varepsilon}$	σk	σk
1.44	1.92	0.09	1.0	1.3

3.6 BOUNDARY CONDITIONS

The following are the boundary conditions used. At the wall no-slip and no-penetration boundary condition ($U_x = 0$, $U_y = 0$) has been used for all the four walls of the tank. For the rotor no slip and no penetration boundary condition ($U_x = 0$, $U_y = 0$) has been used. An angular velocity of rotor (ω_z) is considered.

3.7 RESIDUALS AND CONVERGENCE

All the scaled residuals value (i.e. continuity, x-velocity, y-velocity, z-velocity, k and ε) for convergence have been set below a sufficiently small value of 10^{-6}.

CHAPTER 4:

RESULTS
&
DISCUSSIONS

Attempt is made to investigate the entrainment phenomena through experimental investigation as well as numerical simulation. The details are given below.

4.1 THROUGH NUMERICAL SIMULATION

The results obtained through the numerical calculations for the present problem along with their discussions are described below. All the numerical simulation except one have been performed for water-diesel fluid pair. Only for one case the fluid pair is considered as water-engine oil.

4.1.1 Grid Independence Test

Grid indepence test has been performed to understand the effect of number of grids on the results obtained. It helps to select the optimum mesh size to reduce the computational time.

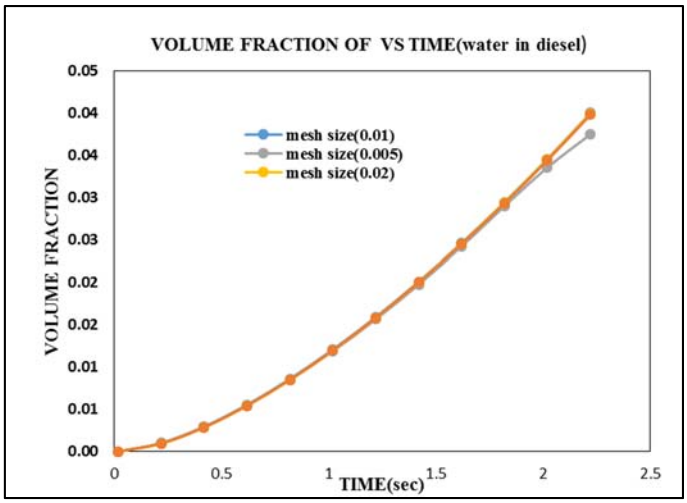

Figure 4.1: Variation of VF of water entrained in to diesel for different grid sizes.

The Figure 4.1 and Figure 4.2 shows the variation of 'VF of water entrained in to the diesel' and 'VF of diesel entrained in to the water' respectively with time for different grid size by keeping all the other parameters fixed. Three grid sizes were considered for meshing (0.005 m, 0.01 m, 0.02 m) and the VF was plotted against time.

From grid independence test 0.01 m grid was chosen as the optimum grid size for meshing.

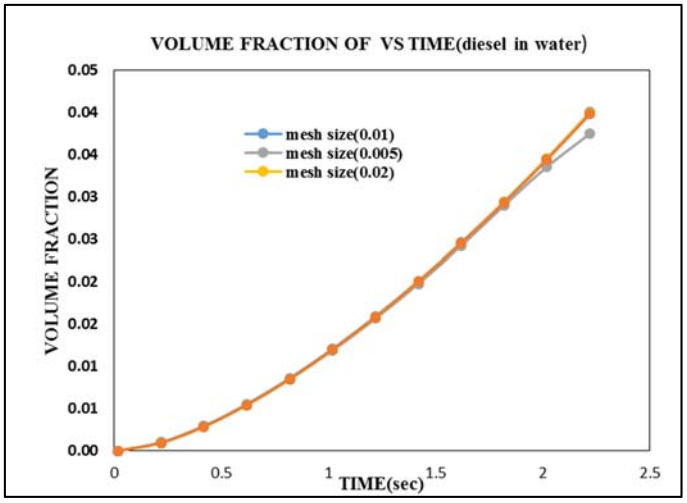

Figure 4.2: Variation of VF of diesel entrained in to water for different grid sizes.

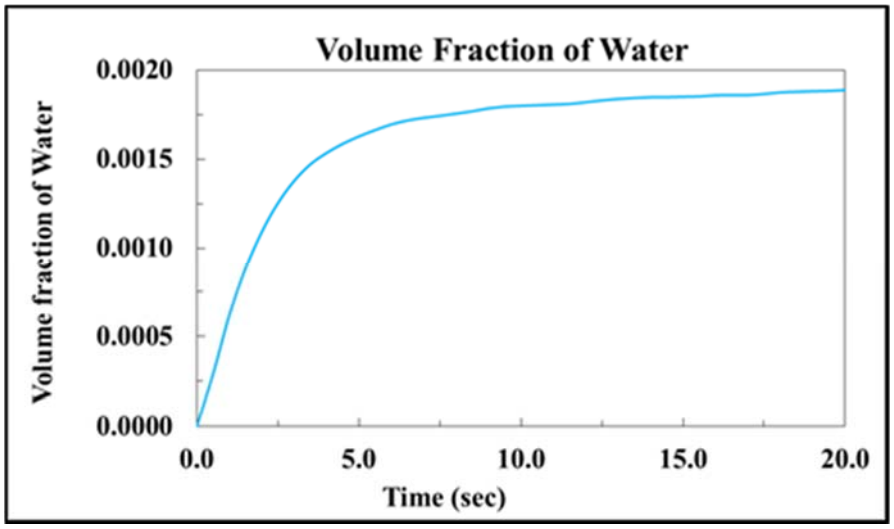

Figure 4.3: Variation of water VF with respect to time for h = 0.05 m, d = 0.1 m, ω = 10 rad/s, Fluid pair = Water-Diesel.

4.1.2 Simulation with h = 0.05 m, d = 0.1 m, ω = 10 rad/s.

For this case, the fluid pair is considered as water-diesel. Here, the rotor diameter (d) is considered as 0.1 m, rotational speed of the rotor (ω) is considered as 10 rad/s, the

distance between the interface and the top of the rotor (h) is considered as 0.05 m. The Figure 4.3 shows the variation of VF of water entrained in diesel with respect to time. In this case the rotor speed and the rotor diameter are very small, so the values of the volume fraction are very small. Initially very small entrainment occur then it remain almost constant with time. The entrainment is almost neglible here. The Figure 4.4 shows the variation of VF of diesel entrained in water with respect to time.

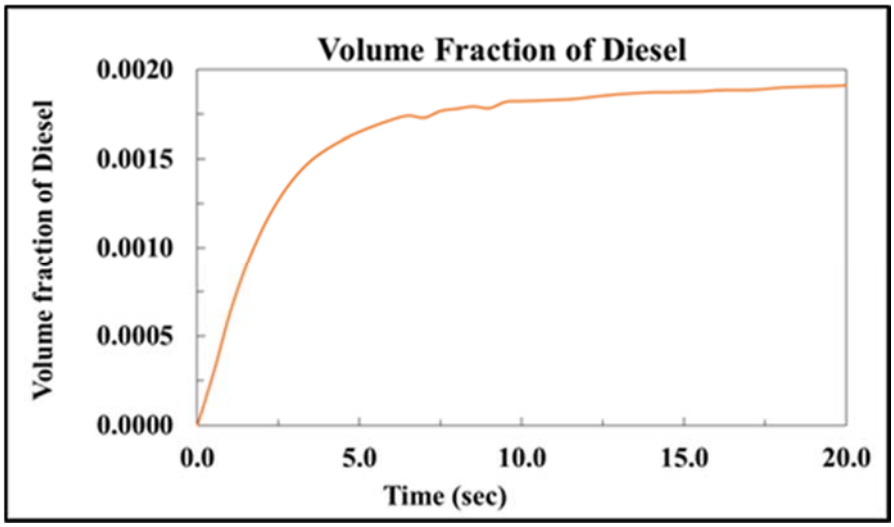

Figure 4.4: Variation of diesel VF with respect to time for h = 0.05 m, d = 0.1 m, ω = 10 rad/s, Fluid pair = Water-Diesel.

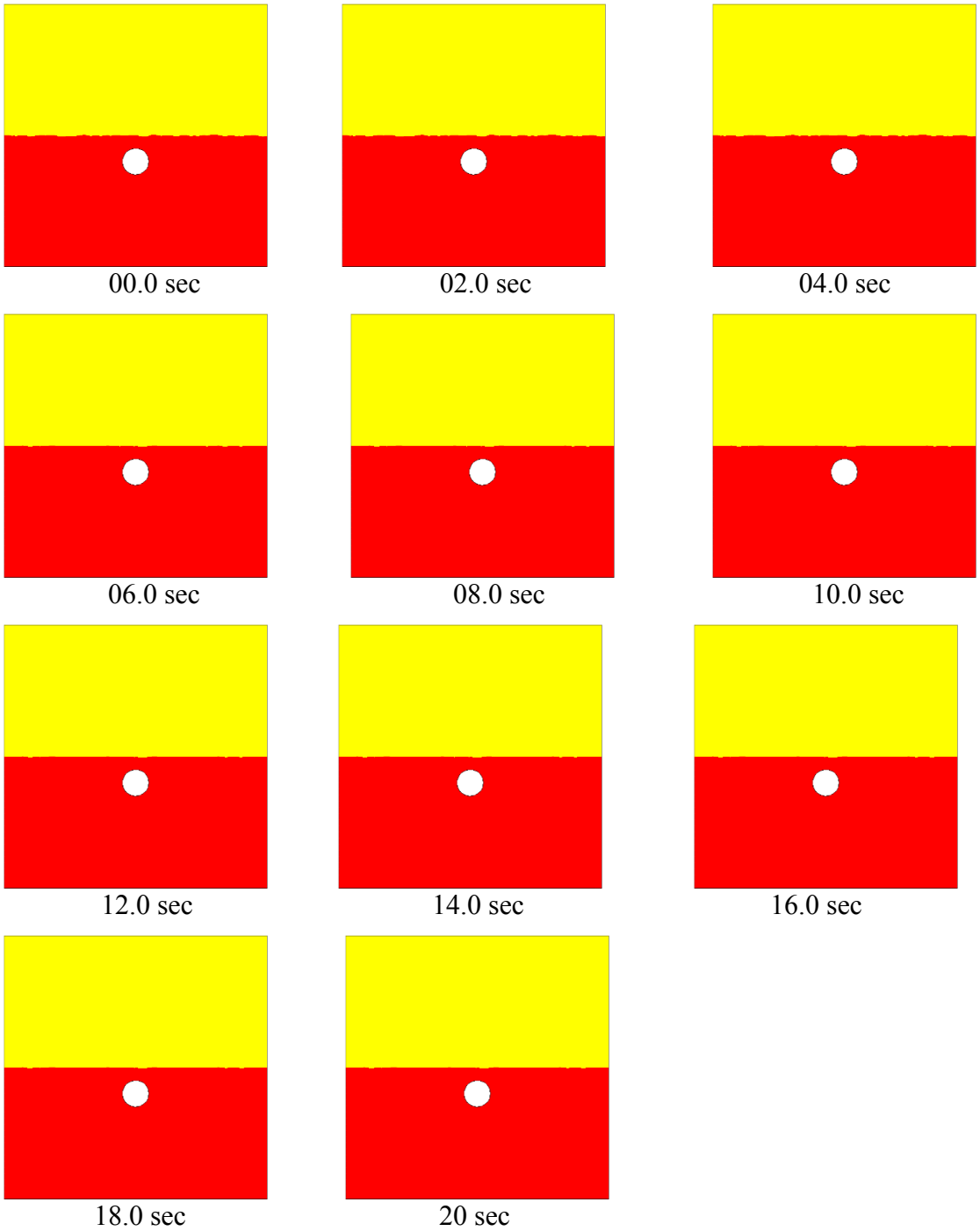

Figure 4.5: The phase contours at different time instants for h = 0.05 m, d = 0.1 m, ω = 10 rad/s, Fluid pair = Water-Diesel.

The Figure 4.5 shows the phase contours of diesel and water for the present case at different time instants. In this case the rotor diameter and the rotor speed are very low and also the rotor is placed below the interface of the two fluids as a result no observable entrainment is noted.

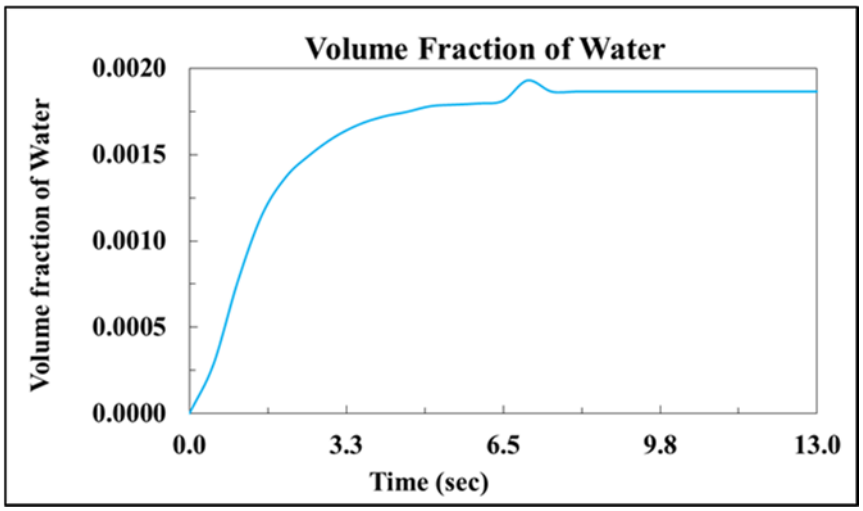

Figure 4.6: Variation of water VF with respect to time for h = 0.1 m, d = 0.2 m, ω = 10 rad/s, Fluid pair = Water-Diesel.

4.1.3 Simulation with h = 0.1 m, d = 0.2 m, ω = 10 rad/s.

For this case, the fluid pair is considered as water-diesel. Here, the rotor diameter (d) is considered as 0.2 m, rotational speed of the rotor (ω) is considered as 10 rad/s, the distance between the interface and the top of the rotor (h) is considered as 0.1 m. Figure 4.6 shows the variation of VF of water entrained into diesel with respect to time. In this case eventhough the rotor diameter is more the rotor speed is very small so the values of the VF entrained are very small. The entrainment is almost negligible here. Figure 4.7 shows the variation of VF of diesel entrained in water with respect to time.

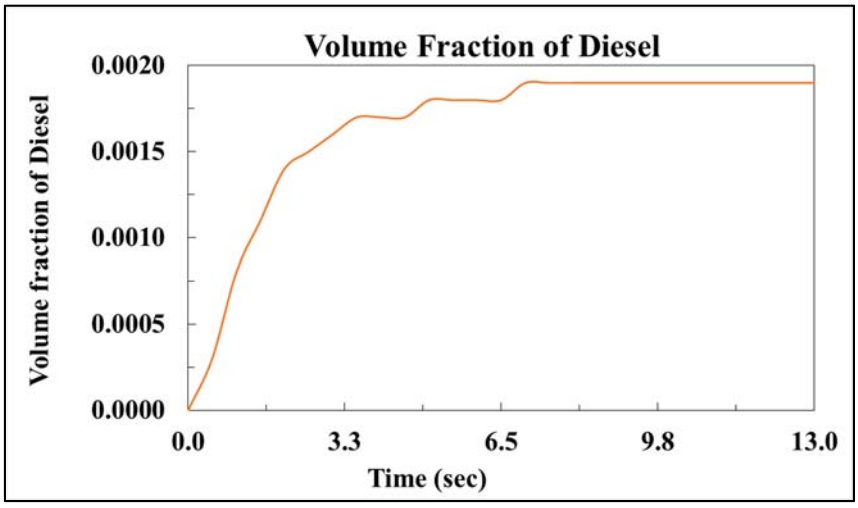

Figure 4.7: Variation of diesel VF with respect to time for h = 0.1 m, d = 0.2 m, ω = 10 rad/s, Fluid pair = Water-Diesel.

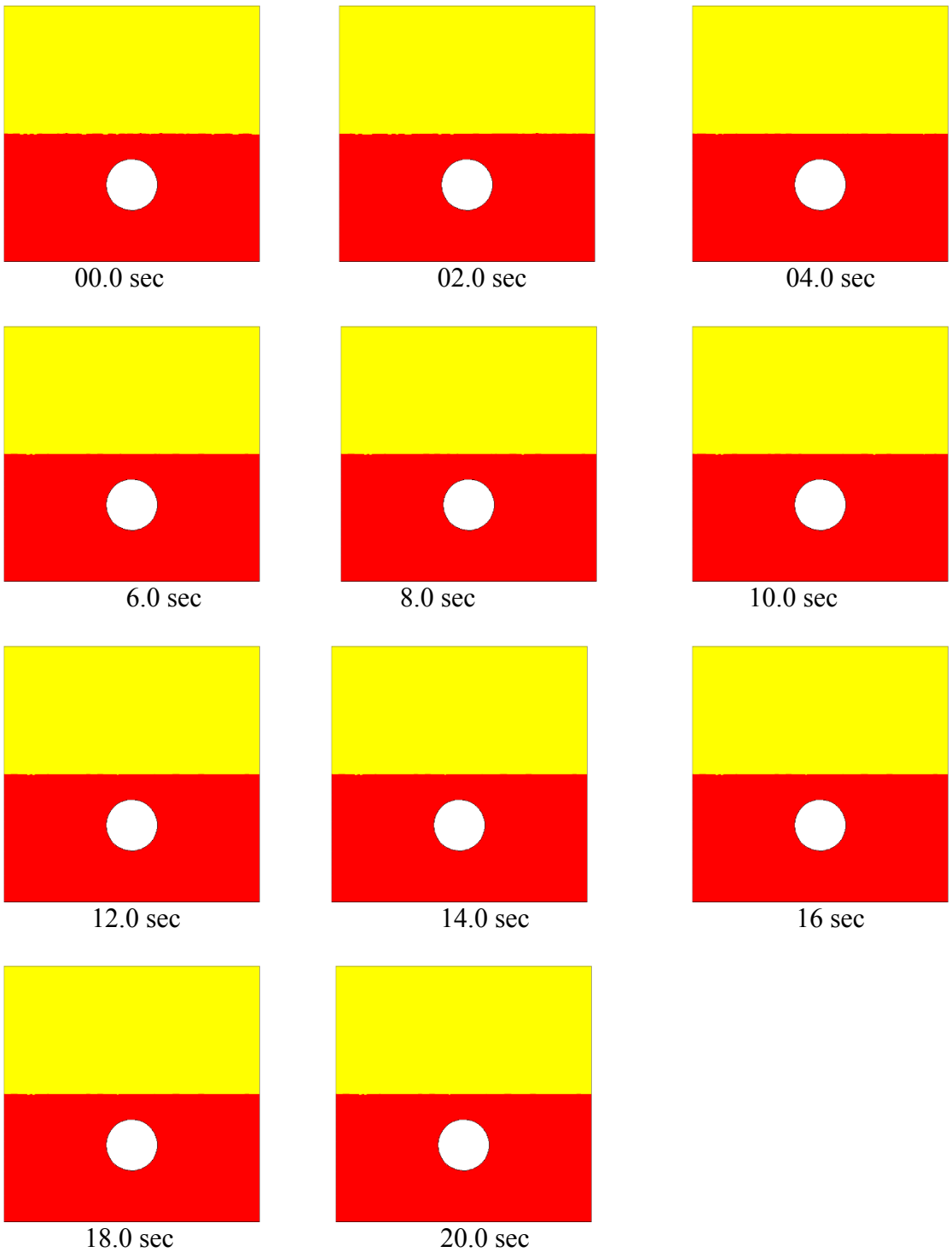

Figure 4.8: The phase contours at different time instants for h = 0.1 m, d = 0.2 m, ω = 10 rad/s, Fluid pair = Water-Diesel.

The Figure 4.8 shows the phase contours at different time instants in the present case. In this case also, no noticeable entrainment is observed because the distance of the rotor from the interface is more.

4.1.4 Simulation with h = 0.05 m, d = 0.2 m, ω = 10 rad/s.

For this case, the fluid pair is considered as water-diesel. Here, the rotor diameter (d) is considered as 0.2 m, rotational speed of the rotor (ω) is considered as 10 rad/s, the distance between the interface and the top of the rotor (h) is considered as 0.05 m. Figure 4.9 shows the variation of VF of water entrained in to diesel with respect to time. In this case the rotor speed is very small and also the rotor is placed below the interface so the values of the VF entrained is very small. The entrainment is almost negligible. Figure 4.10 shows the variation of the VF of diesel entrained in water with time. The Figure 4.11 shows phase contours at different time instants. In this case the entrainment is negligible as the rotor is rotating at very low speed.

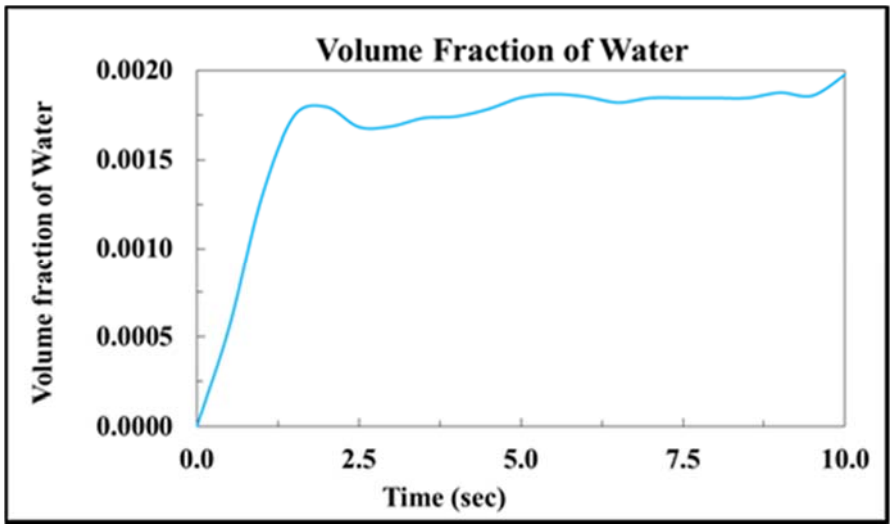

Figure 4.9: Variation of water VF with respect to time for h = 0.05 m, d = 0.2 m, ω = 10 rad/s, Fluid pair = Water-Diesel.

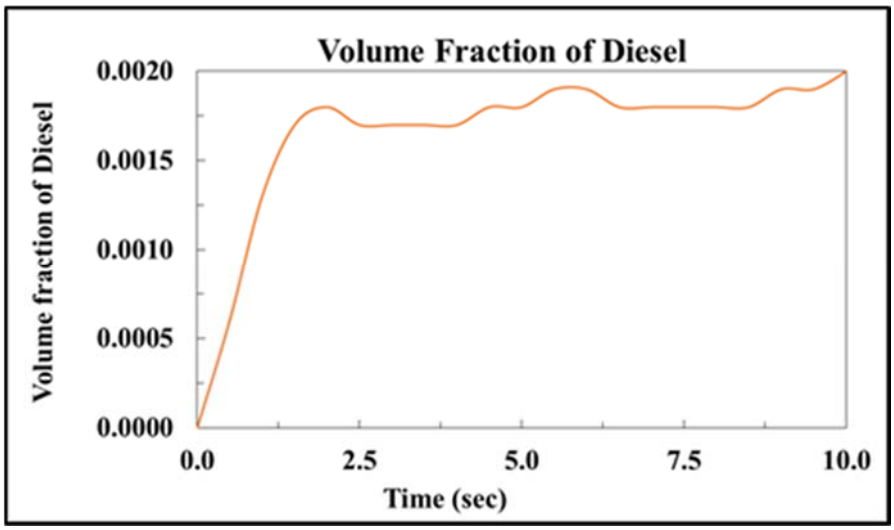

Figure 4.10: Variation of diesel VF with respect to time for h = 0.05 m, d = 0.2 m, ω = 10 rad/s, Fluid pair = Water-Diesel.

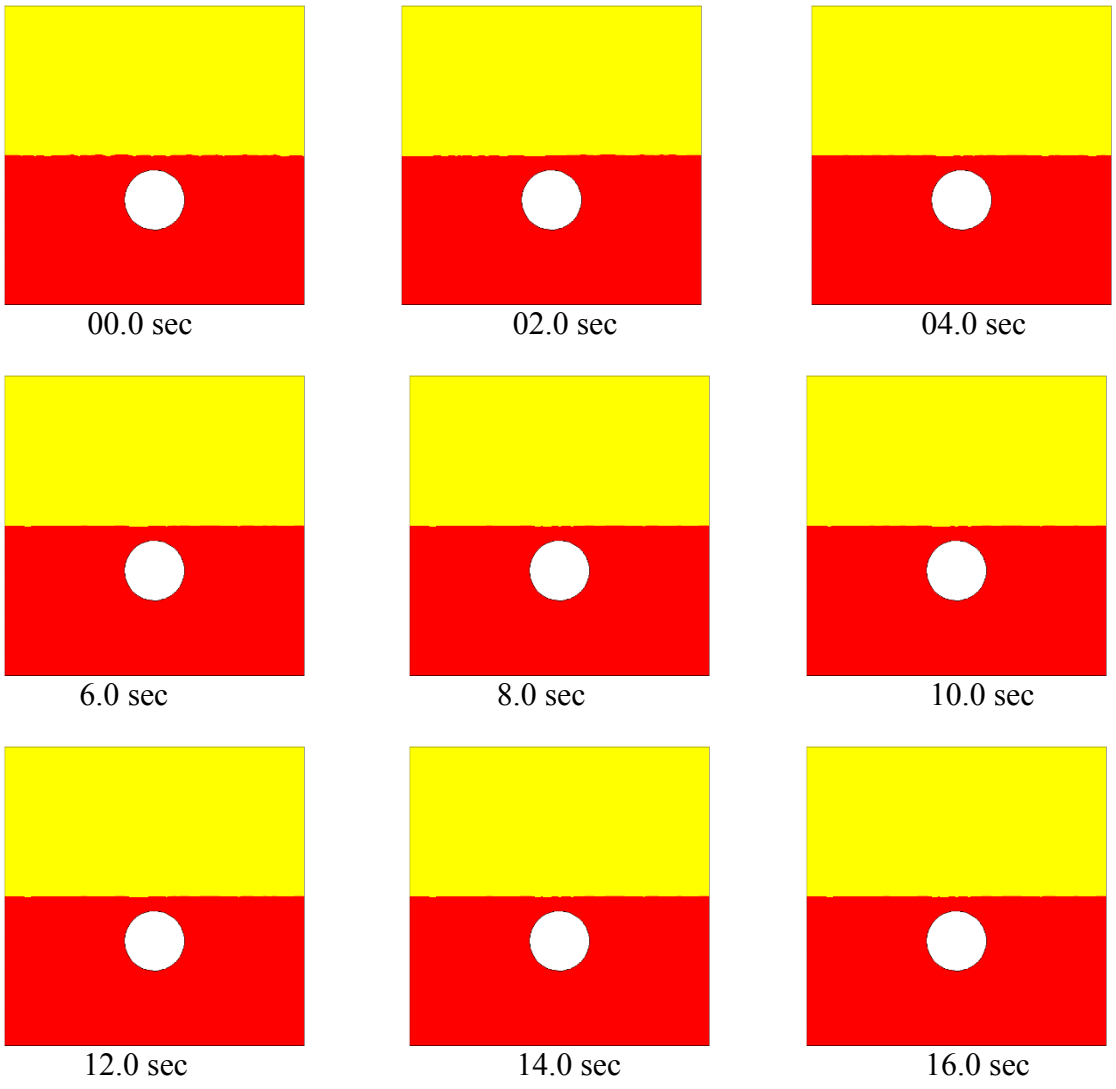

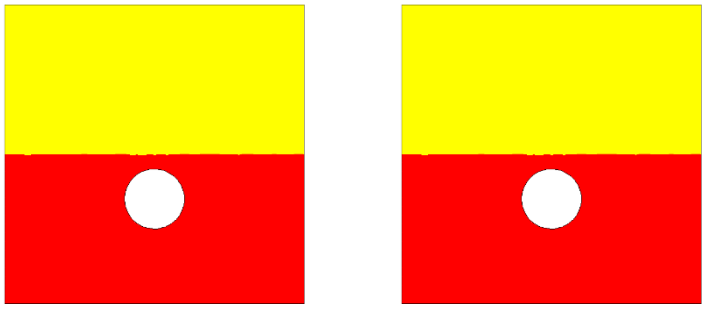

18.0 sec 20.0 sec

Figure 4.11: The phase contours at different time instants for h = 0.05 m, d = 0.2 m, ω = 10 rad/s, Fluid pair = Water-Diesel.

`

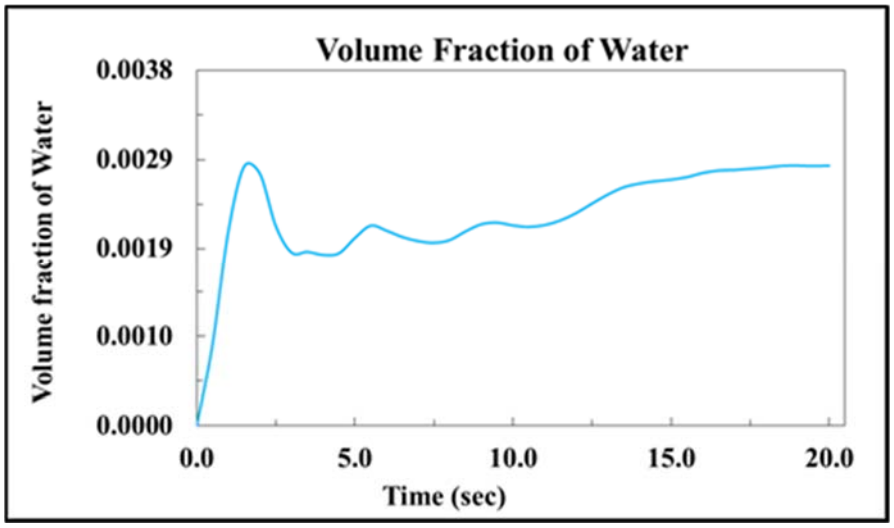

Figure 4.12: Variation of water VF with respect to time for h = 0.05 m, d = 0.2 m, ω = 20 rad/s, Fluid pair = Water-Diesel.

4.1.5 Simulation with h = 0.05 m, d = 0.2 m, ω = 20 rad/s.

For this case, the fluid pair is considered as water-diesel. Here, the rotor diameter (d) is considered as 0.2 m, rotational speed of the rotor (ω) is considered as 20 rad/s, the distance between the interface and the top of the rotor (h) is considered as 0.05 m.The Figure 4.12 shows the variation of VF of water entrained into diesel with respect to time. In this case the rotor speed is very small so the values of the volume fraction is very small. The VF entrained is observed to increase at starting time. And after wards

it remains almost constant. The entrainment is negligible here. Figure 4.13 shows the variation of VF of diesel entrained in water with respect to time.

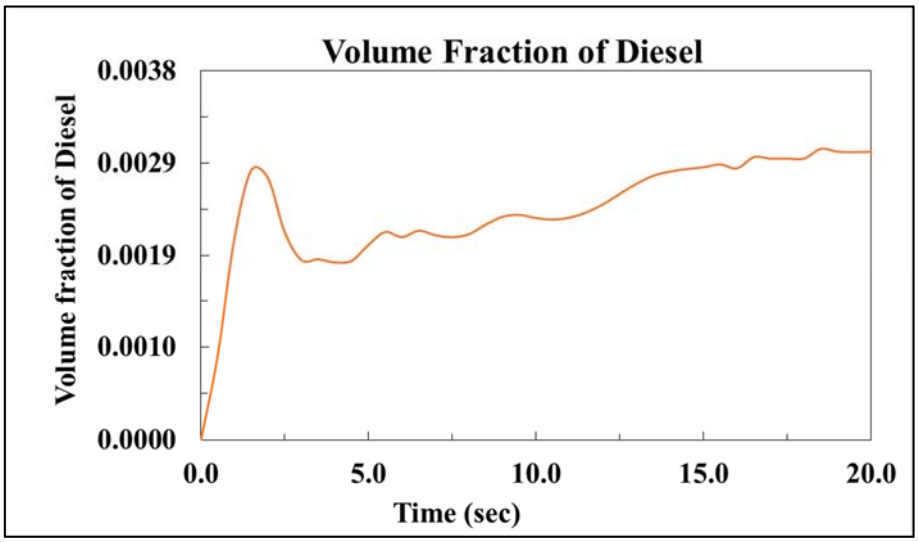

Figure 4.13: Variation of diesel VF with respect to time for h = 0.05 m, d = 0.2 m, ω = 20 rad/s, Fluid pair = Water-Diesel.

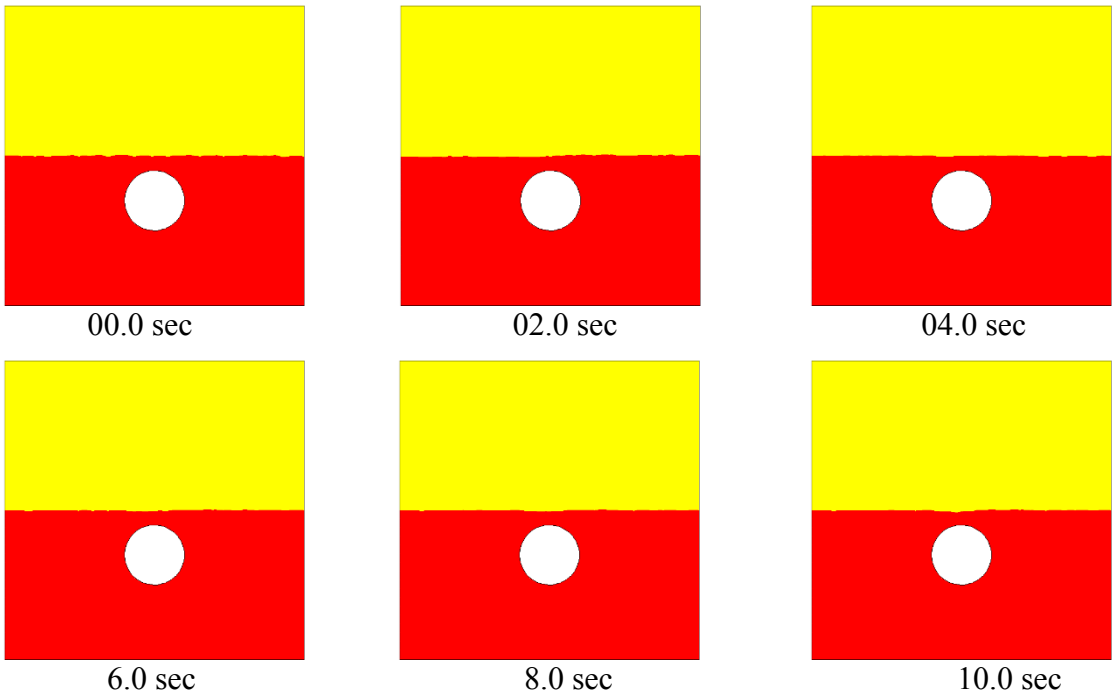

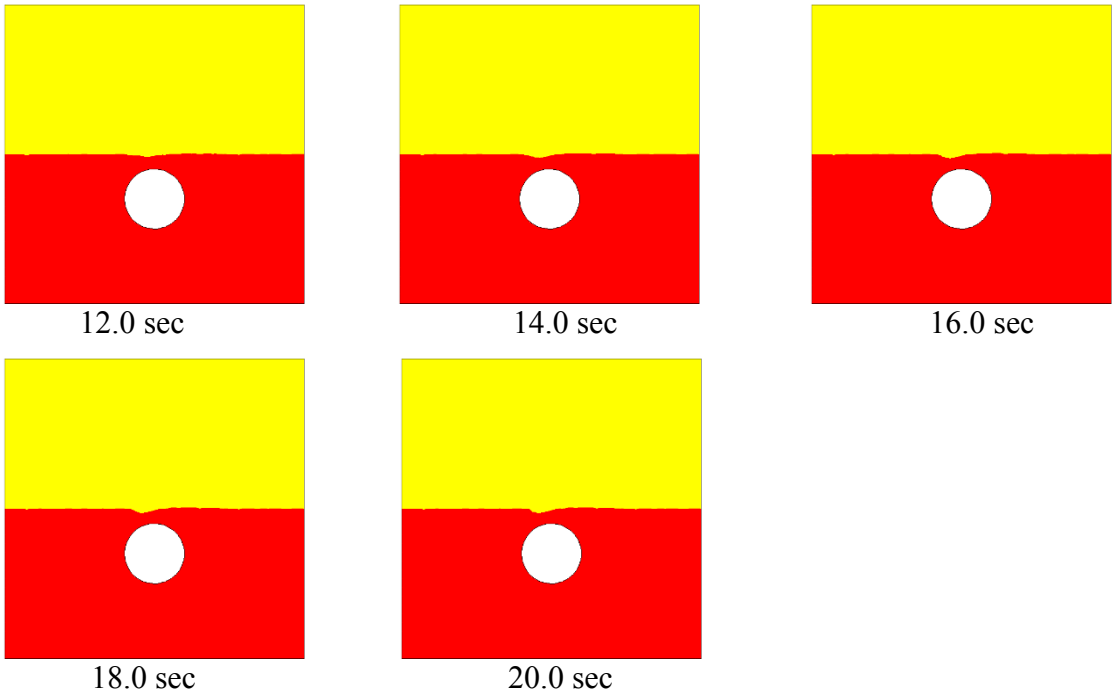

Figure 4.14: The phase contours at different time instants for h = 0.05 m, d = 0.2 m, ω = 20 rad/s, Fluid pair = Water-Diesel.

The Figure 4.14 shows the phase contours at different time instants. In this case slight entrainment is observed . In this case the rotor diameter is higher as a result the rotor is capable of entraining the liquid. But very small amount of entrainment is observed in this case.

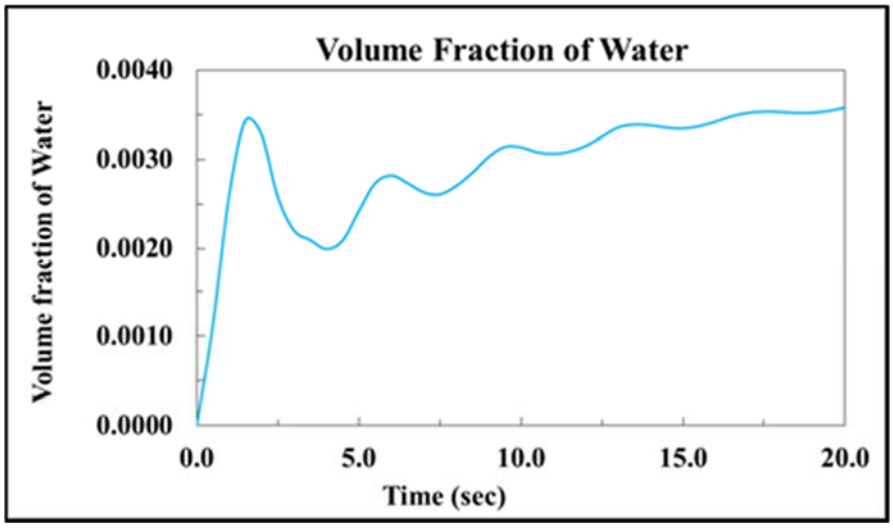

Figure 4.15: Variation of water VF with respect to time for h = 0.025 m, d = 0.2 m, ω = 20 rad/s, Fluid pair = Water-Diesel.

4.1.6 Simulation with h = 0.025 m, d = 0.2 m, ω = 20 rad/s.

For this case, the fluid pair is considered as water-diesel. Here, the rotor diameter (d) is considered as 0.2 m, rotational speed of the rotor (ω) is considered as 20 rad/s, the distance between the interface and the top of the rotor (h) is considered as 0.025 m.The Figure 4.15 shows the variation of VF of water entrained into diesel with respect to time. In this case the rotor speed is very small so the values of the entrained volume fraction is quite small. Slight entrainment is observed towards the end. Figure 4.16 shows the variation of VF of diesel entrained in water with respect to time.

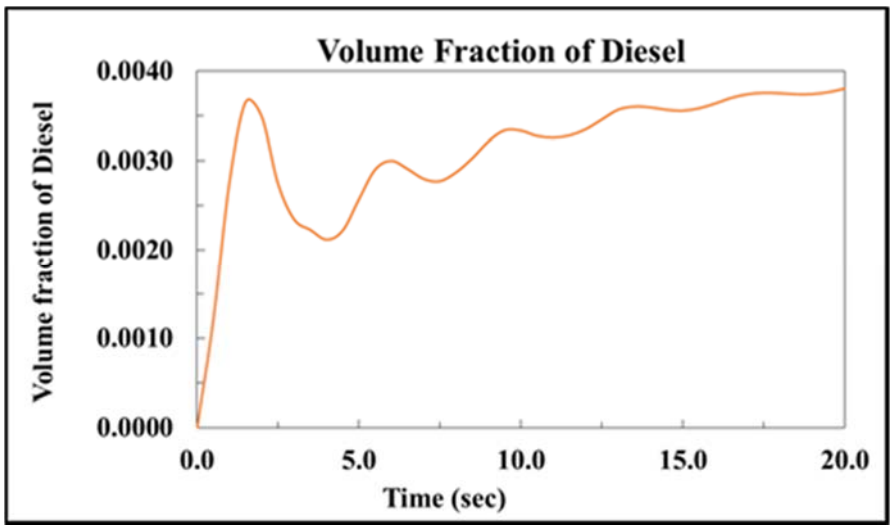

Figure 4.16: Variation of diesel VF with respect to time for h = 0.025 m, d = 0.2 m, ω = 20 rad/s, Fluid pair = Water-Diesel.

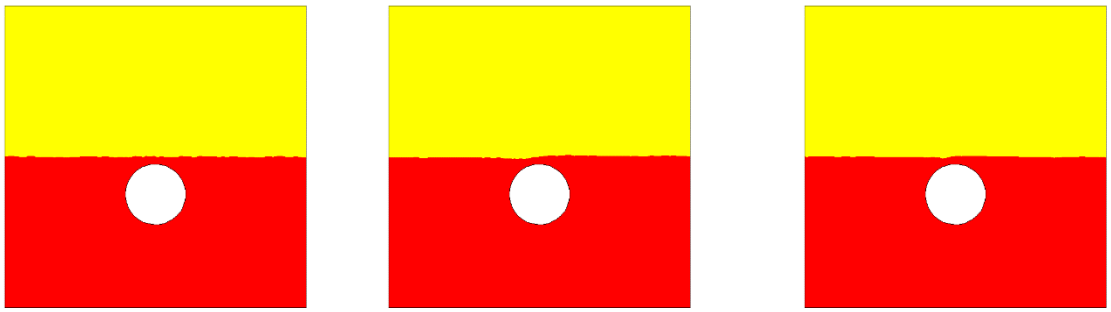

0.0 sec 2.0 sec 4.0 sec

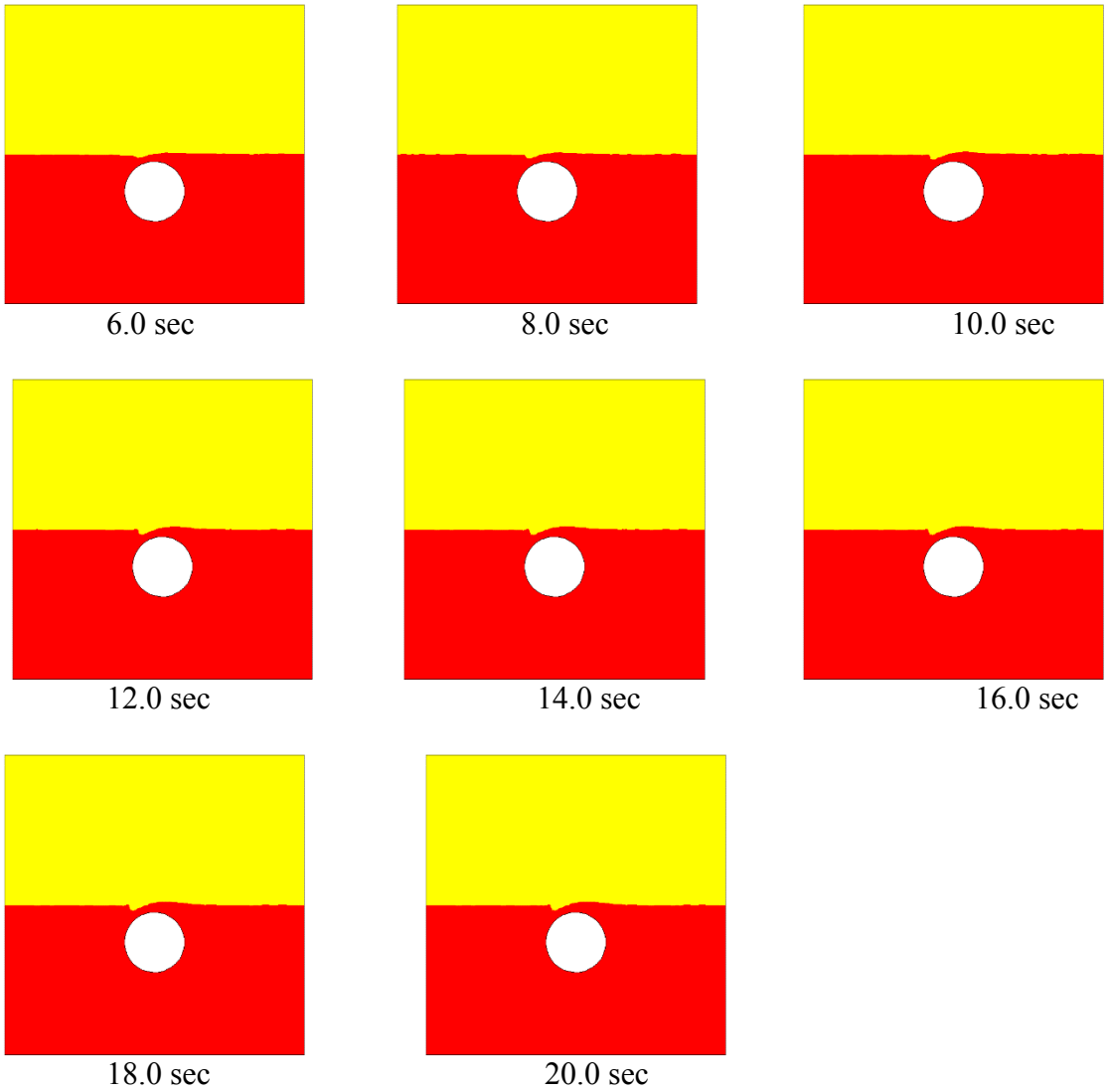

Figure 4.17: The phase contours at different time instants for h = 0.025 m, d = 0.2 m, ω = 20 rad/s, Fluid pair = Water-Diesel.

The Figure 4.17 shows the phase contours at different time instants for the present case. At the beginning no entrainment is seen but slight entrainment of the lighter phase in to the heavier phase is observed.

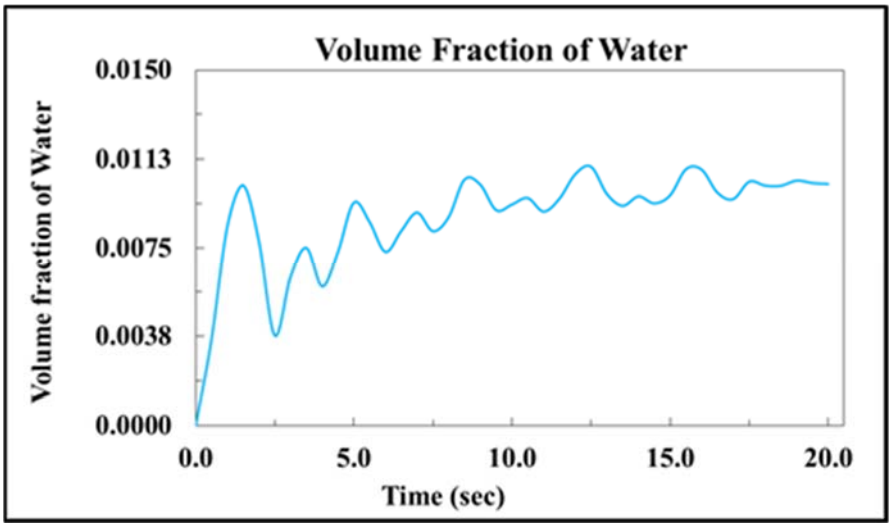

Figure 4.18: Variation of water VF with respect to time for h = 0.2 m, d = 0.4 m, ω = 10 rad/s, Fluid pair = Water-Diesel.

4.1.7 Simulation with h = 0.2 m, d = 0.4 m, ω = 10 rad/s.

For this case, the fluid pair is considered as water-diesel. Here, the rotor diameter (d) is considered as 0.4 m, rotational speed of the rotor (ω) is considered as 10 rad/s, the distance between the interface and the top of the rotor (h) is considered as 0.2 m. The Figure 4.18 shows the Variation of VF of water entrained into diesel with respect to time. In this case the rotor is placed at the interface between the two liquids. As a result the entrainment is observed. But, as the diameter of the rotor is very large, the heavier liquid is unable to climb over the rotor. Figure 4.19 shows the variation of VF of diesel entrained into water with respect to time.

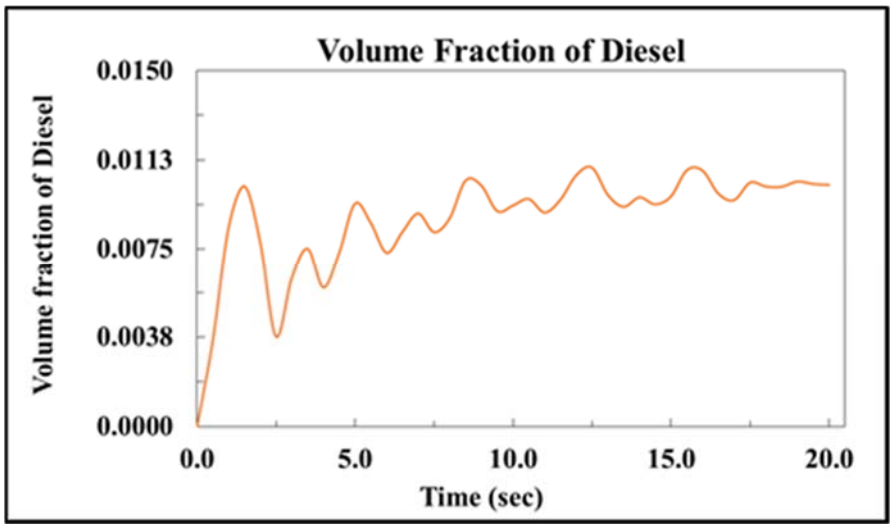

Figure 4.19: Variation of diesel VF with respect to time for h = 0.2 m, d = 0.4 m, ω = 10 rad/s, Fluid pair = Water-Diesel.

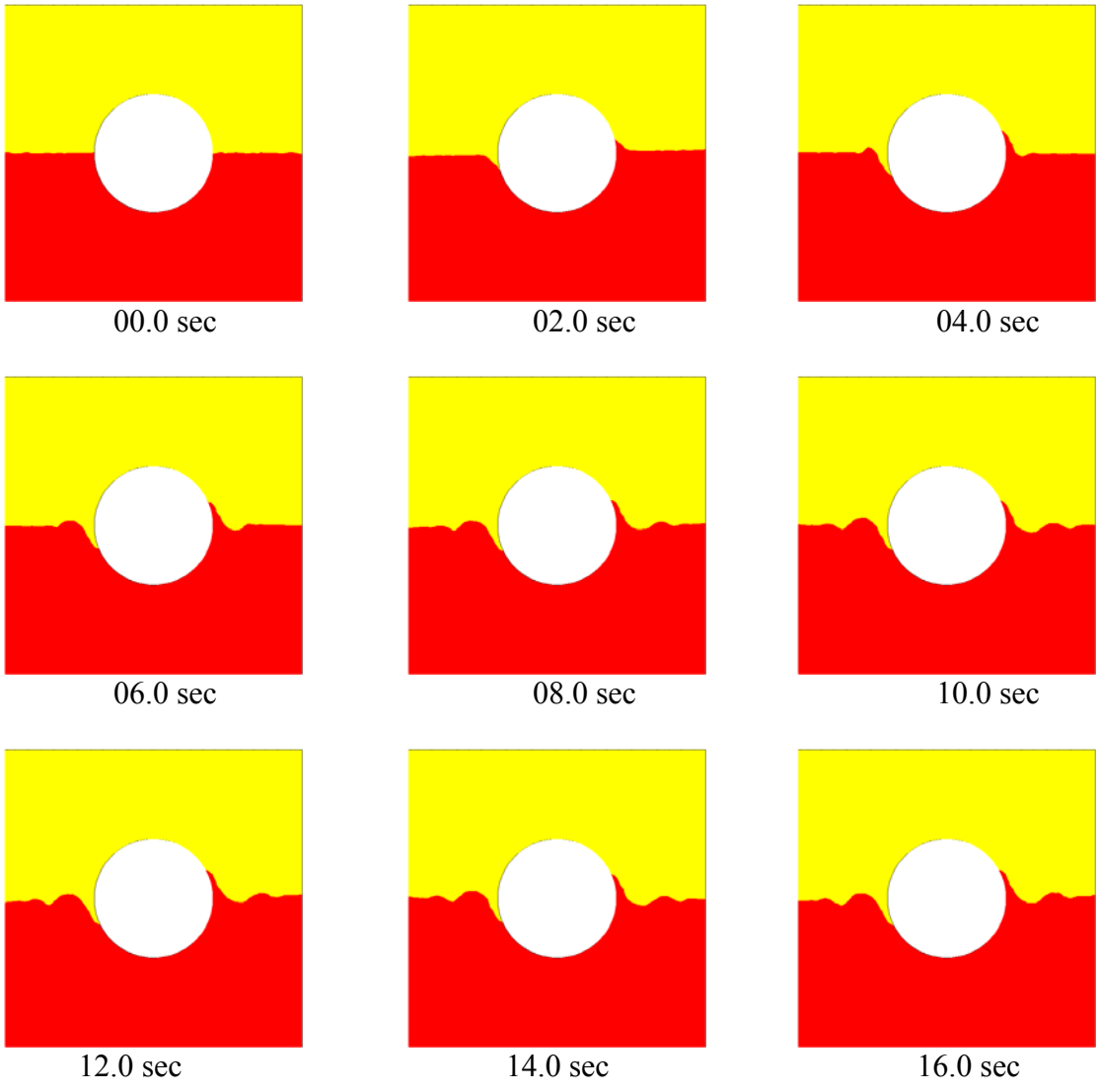

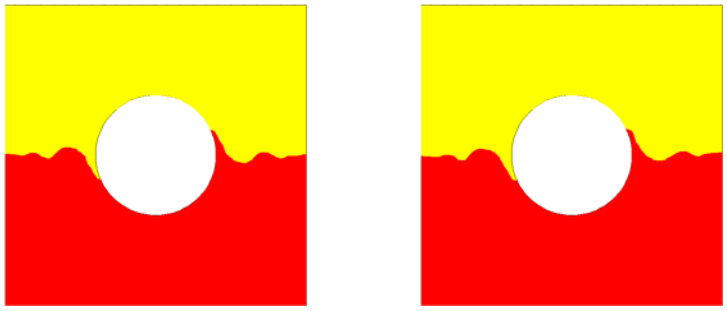

18.0 sec 20.0 sec

Figure 4.20: The phase contours at different time instants for h = 0.2 m, d = 0.4 m, ω = 10 rad/s, Fluid pair = Water-Diesel.

The Figure 4.20 shows the phase contours at different time instants. The size of the rotor is large and the rotor speed is not so high. As a result, the entrainment is not increasing at faster rate as observed initially.

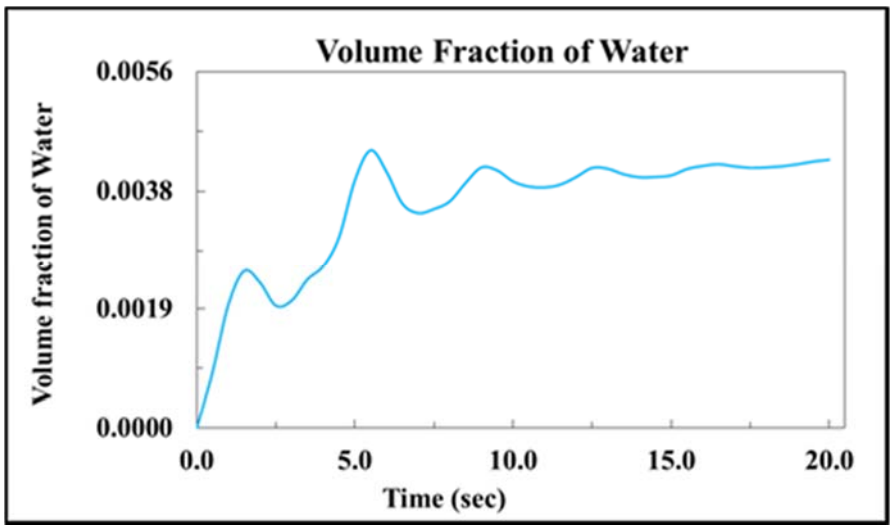

Figure 4.21: Variation of water VF with respect to time for h = 0.05 m, d = 0.1 m, ω = 100 rad/s, Fluid pair = Water-Diesel

4.1.8 Simulation with h = 0.05 m, d = 0.1 m, ω = 100 rad/s.

For this case, the fluid pair is considered as water-diesel. Here, the rotor diameter (d) is considered as 0.1 m, rotational speed of the rotor (ω) is considered as 100 rad/s, the distance between the interface and the top of the rotor (h) is considered as 0.05 m. The Figure 4.21 shows variation of VF of water entrained in to diesel with respect to time. In this case the rotor speed is high and the rotor diameter used is very small so the values of the volume fraction entrained is very small. As the rotor diameter is small it is not able to pull the lighter fluid in to the heavier fluid. Figure 4.22 shows the variation of VF of diesel entrained in water with respect to time.

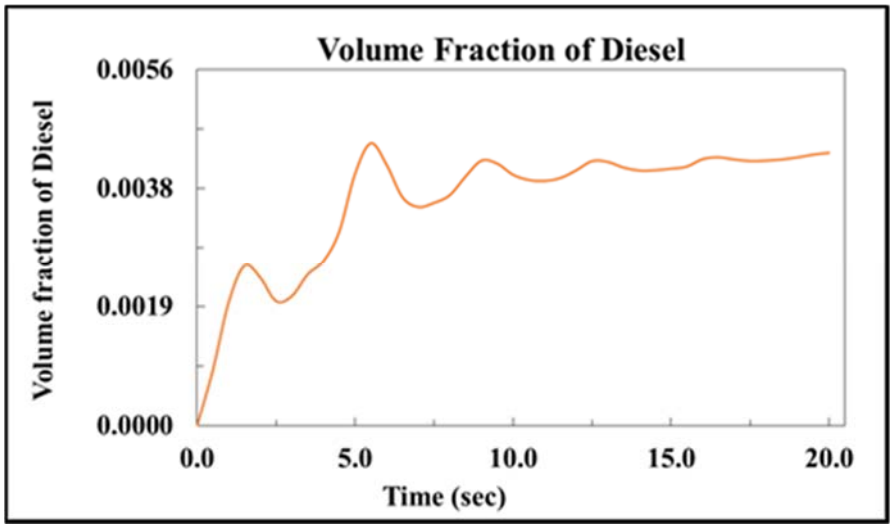

Figure 4.22: Variation of diesel VF with respect to time h = 0.05 m, d = 0.1 m, ω = 100 rad/s, Fluid pair = Water-Diesel.

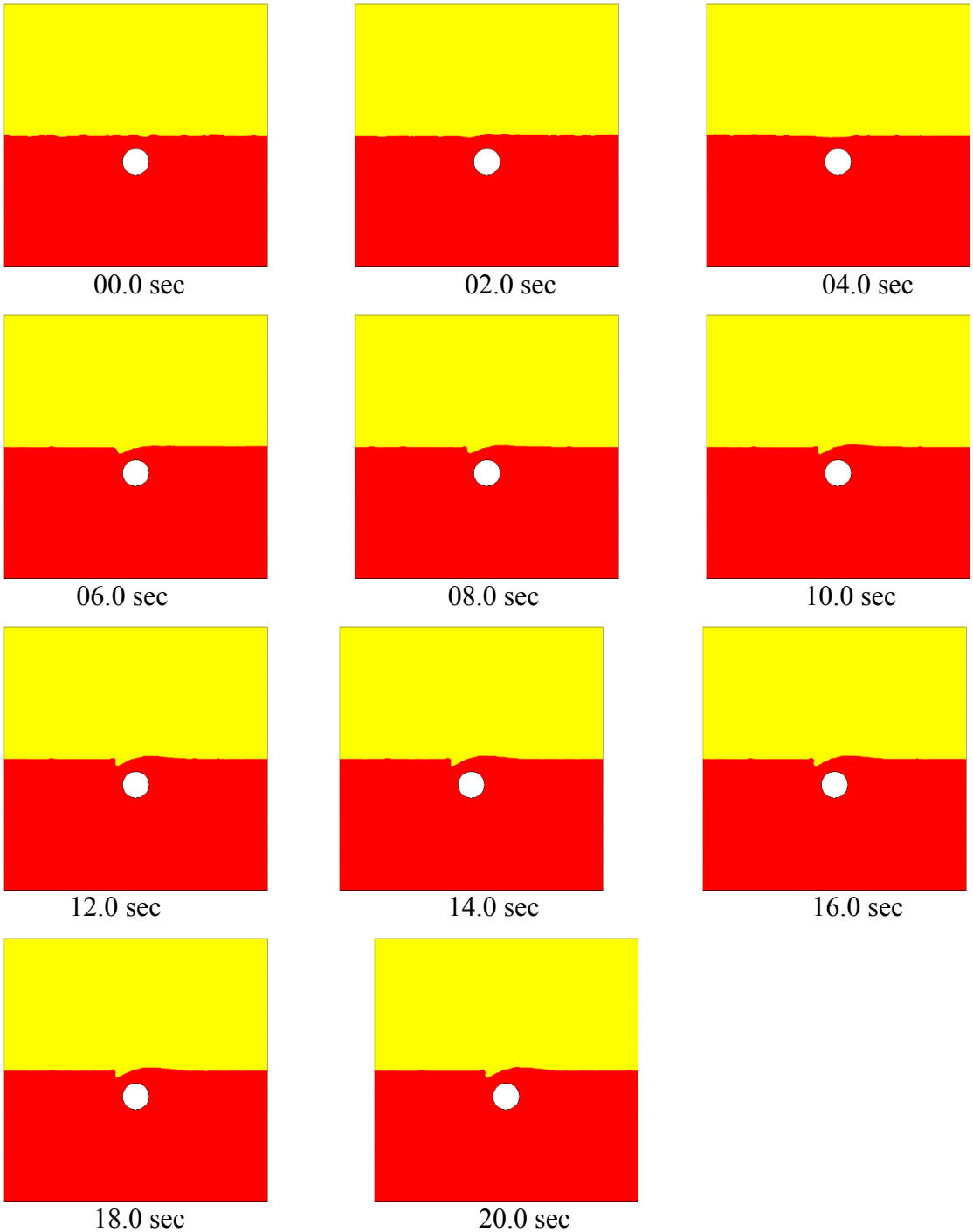

Figure 4.23: The phase contours at different time instants for h = 0.05 m, d = 0.1 m, ω = 100 rad/s, Fluid pair = Water-Diesel.

The Figure 4.23 shows the phase contours at different time instants. Slight entrainment was observable in this case because the rotor speed is higher for this case. As the rotor diameter used is small the rotor is not capable of pulling the lighter phase into the heavier phase.

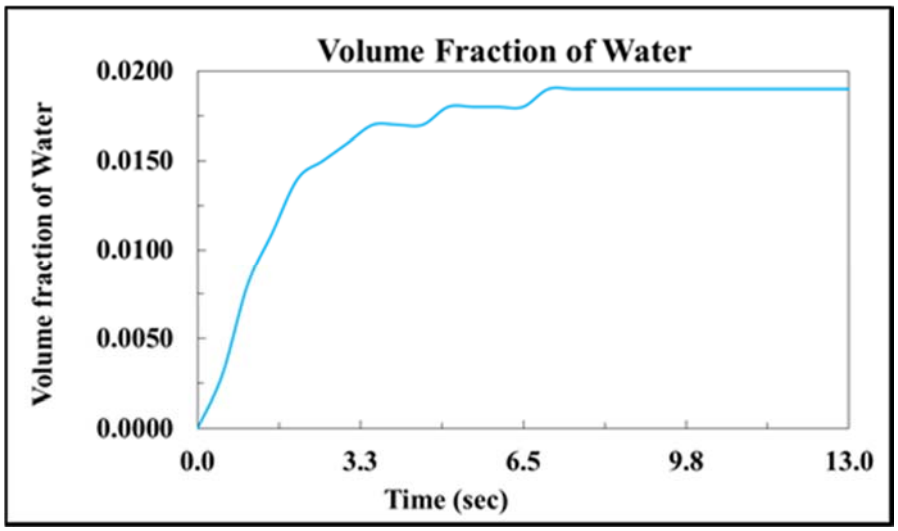

Figure 4.24: Variation of water VF with respect to time for . h = 0.1 m, d = 0.2 m, ω = 50 rad/s, Fluid pair = Water-Diesel.

4.1.9 Simulation with h = 0.1 m, d = 0.2 m, ω = 50 rad/s.

For this case, the fluid pair is considered as water-diesel. Here, the rotor diameter (d) is considered as 0.2 m, rotational speed of the rotor (ω) is considered as 50 rad/s, the distance between the interface and the top of the rotor (h) is considered as 0.1 m. The Figure 4.24 shows the variation of VF of water entrained into diesel with respect to time. In this case the rotor is kept at the interface between the two fluids. Figure 4.25 shows the variation of diesel VF entrained in water with respect to time.

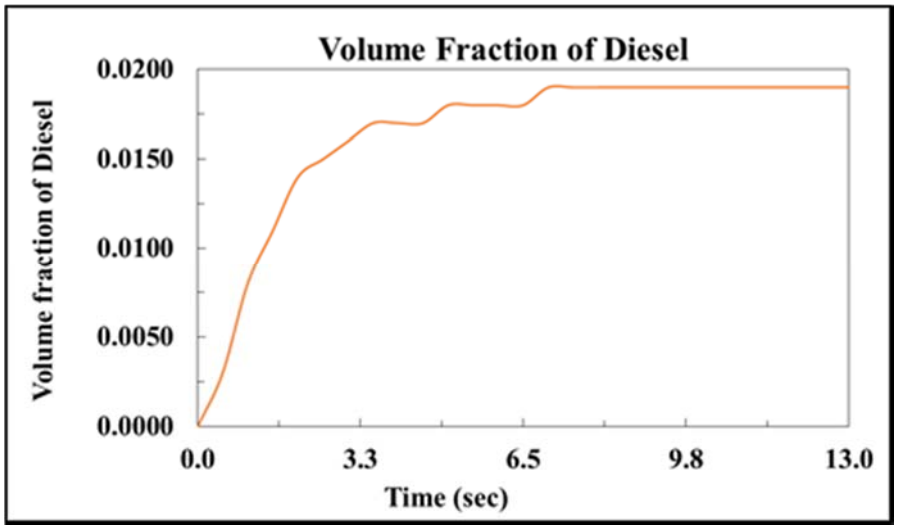

Figure 4.25: Variation of diesel VF with respect to time for . h = 0.1 m, d = 0.2 m, ω = 50 rad/s, Fluid pair = Water-Diesel.

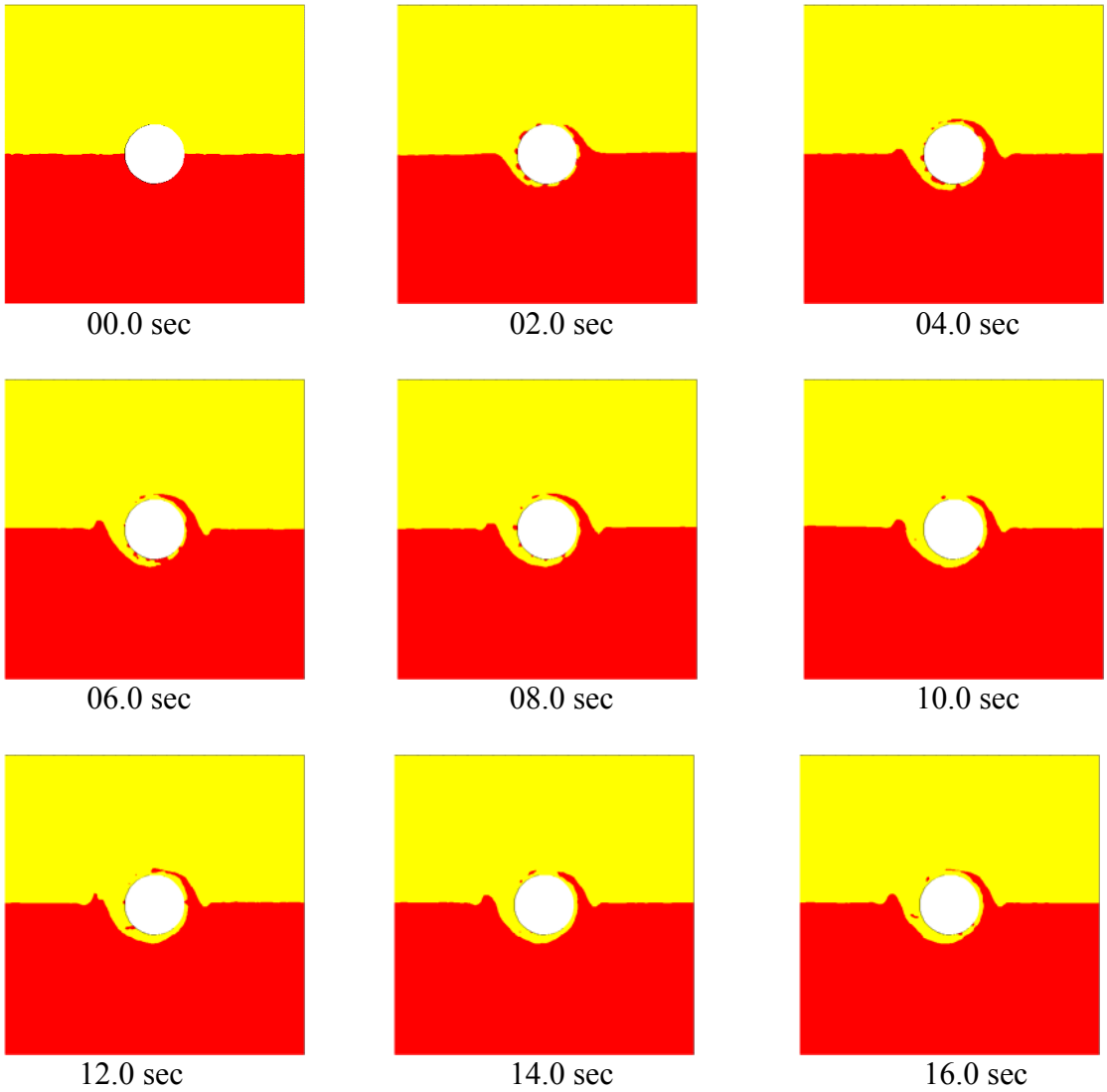

Figure 4.26: The phase contours at different time instants for . h = 0.1 m, d = 0.2 m, ω = 50 rad/s, Fluid pair = Water-Diesel.

The Figure 4.26 shows the phase contours at different time instants for the present cases. In this case very good entrainment is observed as the rotor diameter and rotor speed are suffeciently large and the rotor is placed at the interface of the two fluids.

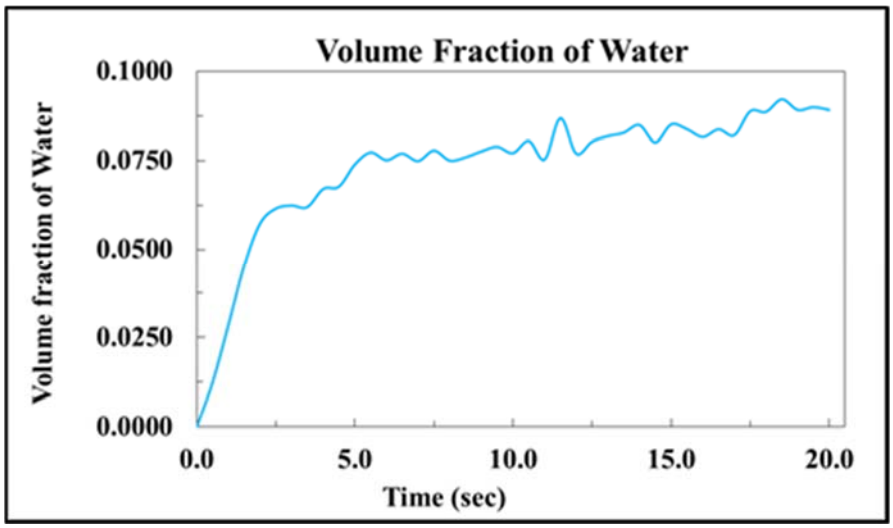

Figure 4.27: Variation of water VF with respect to time for h = 0.015 m, d = 0.2 m, ω = 200 rad/s, Fluid pair = Water-Diesel.

4.1.10 Simulation with h = 0.015 m, d = 0.2 m, ω = 200 rad/s.

For this case, the fluid pair is considered as water-diesel. Here, the rotor diameter (d) is considered as 0.2 m, rotational speed of the rotor (ω) is considered as 200 rad/s, the distance between the interface and the top of the rotor (h) is considered as 0.015 m. The Figure 4.27 shows variation of VF of water entrained in to diesel with respect to time. In this case the rotor speed is high and the distance from the interface to the rotor top is small as a result very good entrainment is observed. Figure 4.28 shows the variation of VF of diesel entrained into water with respect to time.

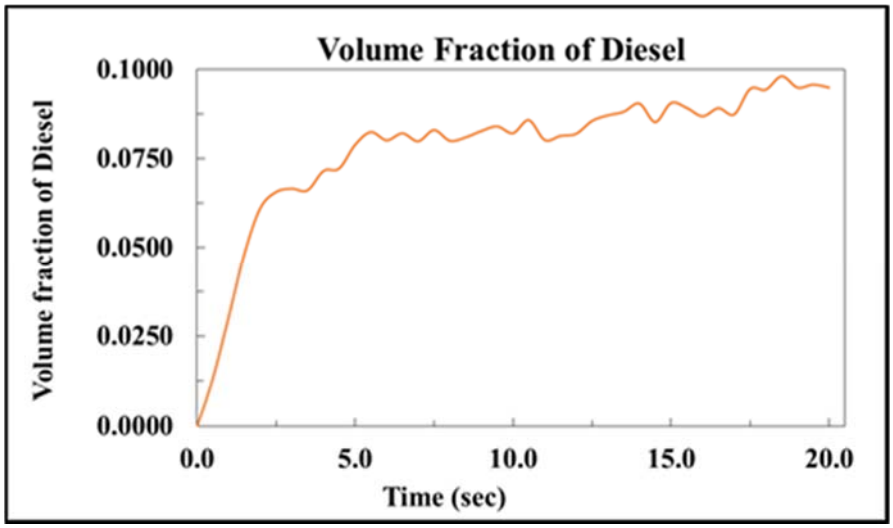

Figure 4.28: Variation of diesel VF with respect to time for h = 0.015 m, d = 0.2 m, ω = 200 rad/s, Fluid pair = Water-Diesel.

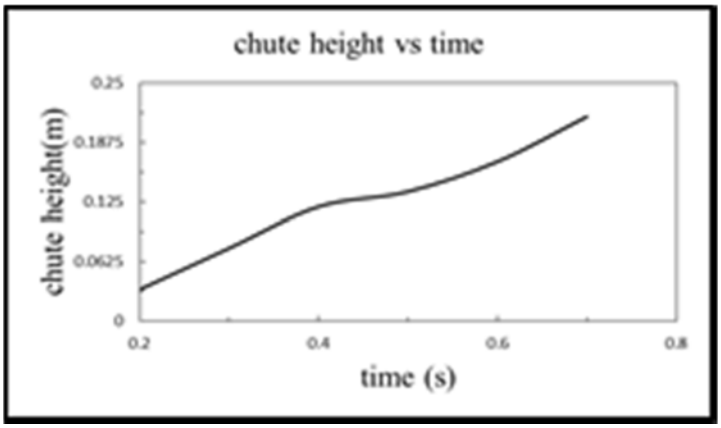

Figure 4.29: Variation of chute height with respect to time for h = 0.015 m, d = 0.2 m, ω = 200 rad/s, Fluid pair = Water-Diesel.

The Figure 4.29 shows the variation of chute height with respect to time. The chute height is increasing with time as more and more liquid gets entrained in to each other with time due to increased rotor speed and decreased distance of rotor from the interface. The Figure 4.30 shows the phase contours at different time instants for the present case.

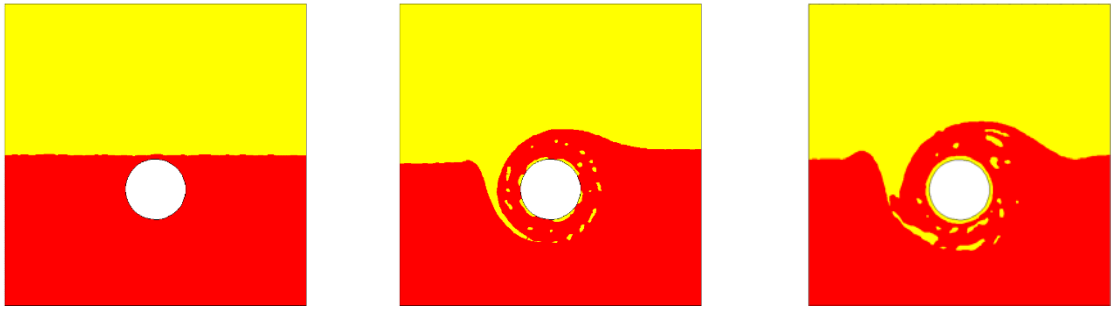

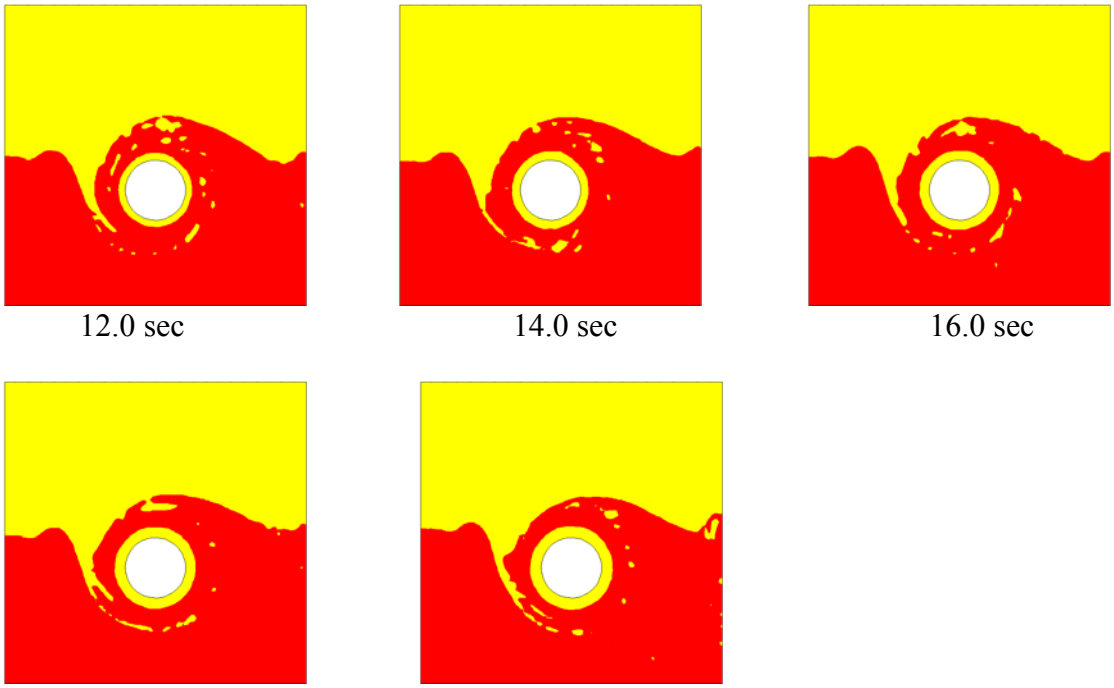

Figure 4.30: The phase contours at different time instants for h = 0.015 m, d = 0.2 m, ω = 200 rad/s, Fluid pair = Water-Diesel.

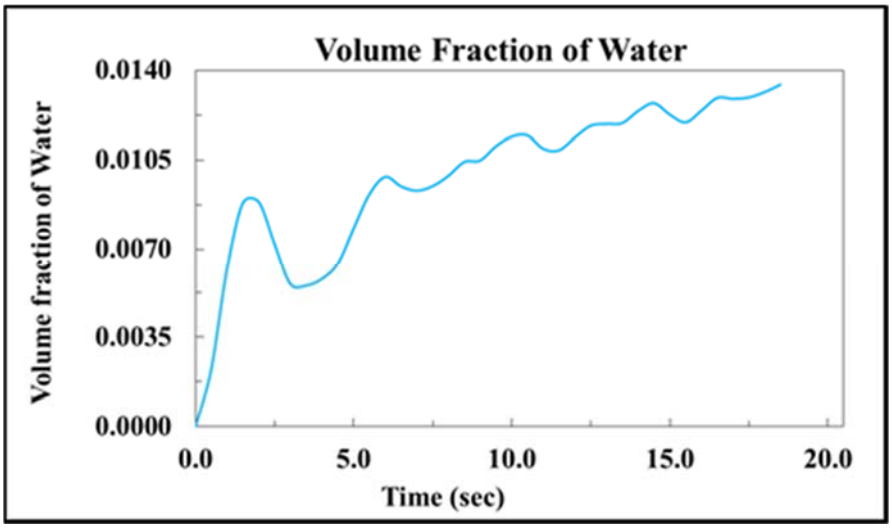

Figure 4.31: Variation of water VF with respect to time for h = 0.025 m, d = 0.2 m, ω = 50 rad/s, Fluid pair = Water-Diesel.

4.1.11 Simulation with h = 0.025 m, d = 0.2 m, ω = 50 rad/s.

For this case, the fluid pair is considered as water-diesel. Here, the rotor diameter (d) is considered as 0.2 m, rotational speed of the rotor (ω) is considered as 50 rad/s, the distance between the interface and the top of the rotor (h) is considered as 0.025 m. The

Figure 4.31 shows variation of VF of water entrained into diesel with respect to time. In this case the volume fraction entrained is observed to increase with time as the rotor is placed near the interface and the rotor speed is sufficently high and the rotor diameter is also not so small. Figure 4.32 shows the variation of the VF of diesel entrained in to water with respect to time.

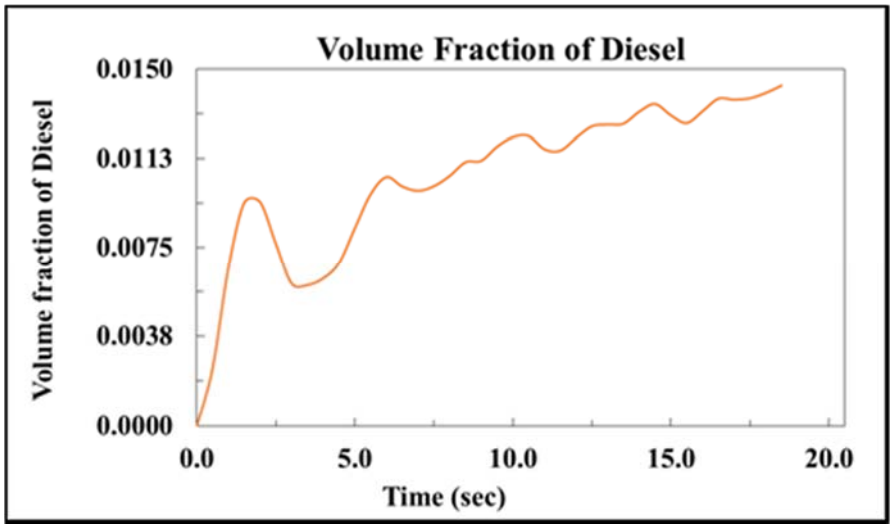

Figure 4.32: Variation of diesel VF with respect to time for h = 0.025 m, d = 0.2 m, ω = 50 rad/s, Fluid pair = Water-Diesel.

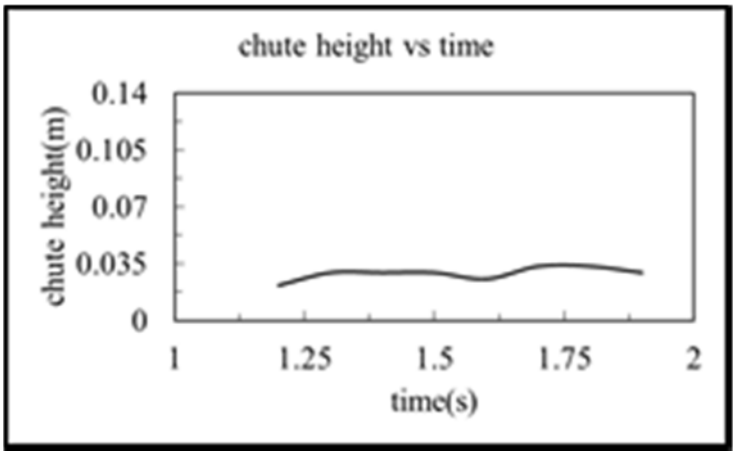

Figure 4.33: variation of chute height with time for h = 0.025 m, d = 0.2 m, ω = 50

The Figure 4.33 shows the variation of chute height with respect to time. The chute remains constant with time.

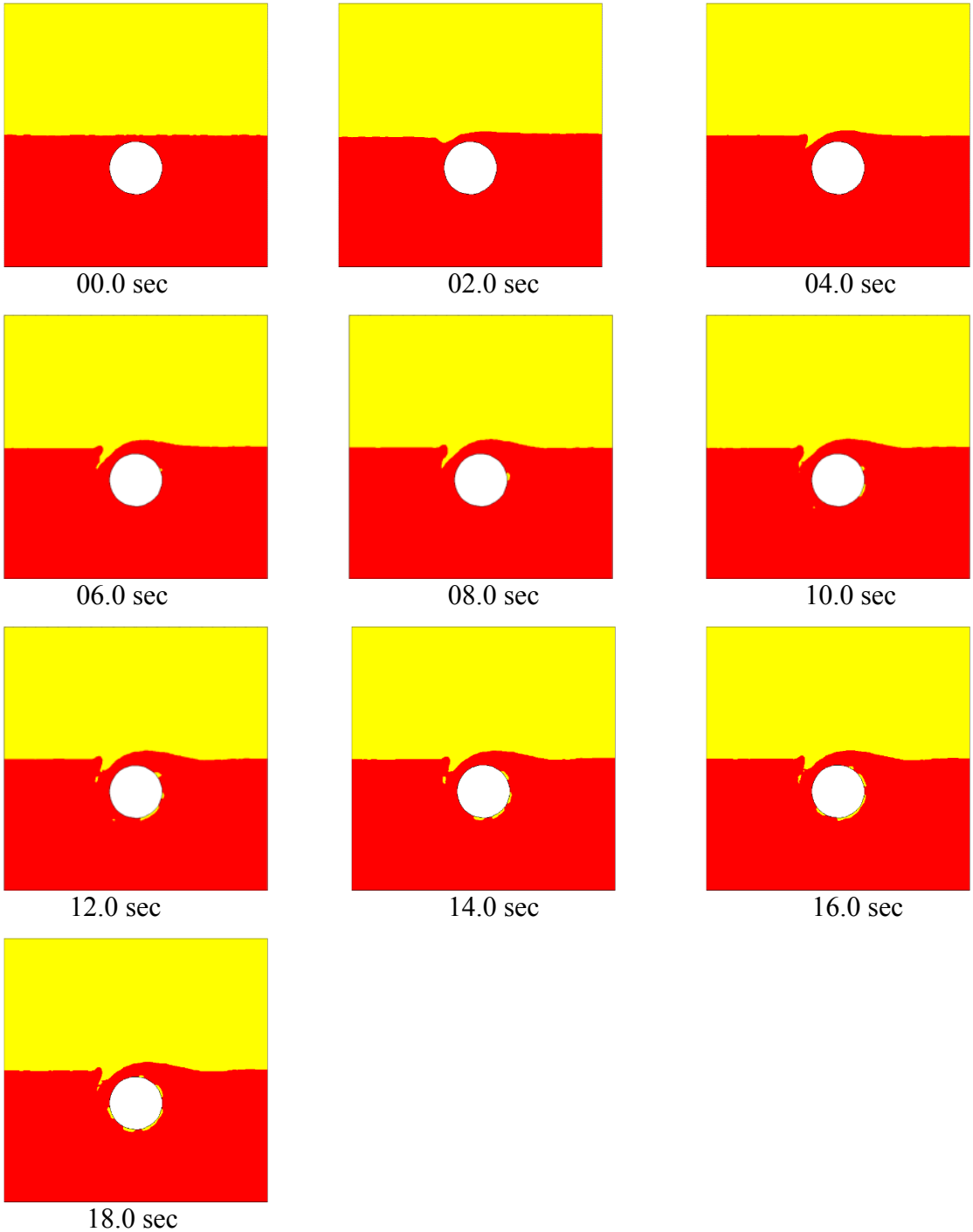

Figure 4.34: The phase contours at different time instants for h = 0.025 m, d = 0.2 m, ω = 50 rad/s, Fluid pair = Water-Diesel.

The Figure 4.34 shows the phase contours at different time instants. In this case good entrainment is observed. The rotor is able to entrain the fluids as the rotor speed is high, the distance from the interface is small and diameter of rotor is sufficently large.

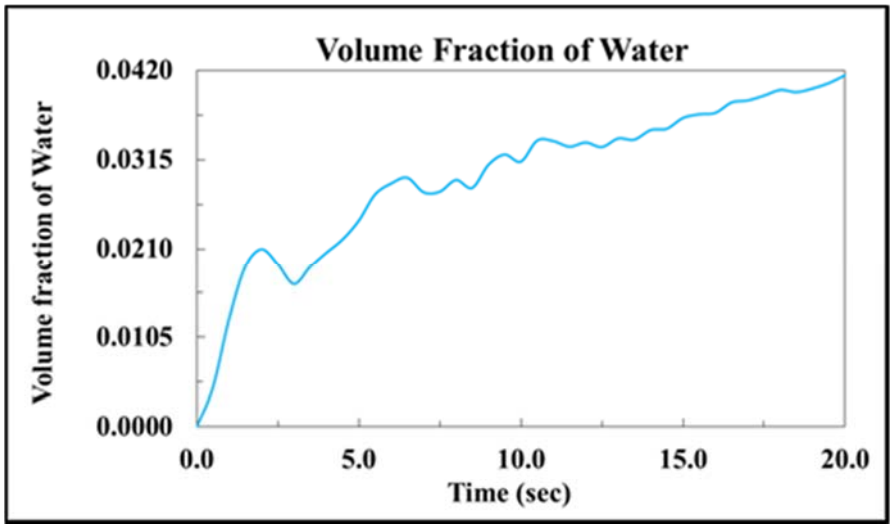

Figure 4.35: Variation of water VF with respect to time for h = 0.025 m, d = 0.2 m, ω = 100 rad/s, Fluid pair = Water-Diesel.

4.1.12 Simulation with h = 0.025 m, d = 0.2 m, ω = 100 rad/s.

For this case, the fluid pair is considered as water-diesel. Here, the rotor diameter (d) is considered as 0.2 m, rotational speed of the rotor (ω) is considered as 100 rad/s, the distance between the interface and the top of the rotor (h) is considered as 0.025 m. The Figure 4.35 shows the Variation of VF of water entrained inti diesel with respect to time. In this case it has been observed that the volume fraction is increases at a faster rate. This is because the rotor speed is high, the distance of the rotor from the interface is small and the rotor diameter is sufficiently large. The Figure 4.36 shows the variation of VF of diesel entrained in to water with respect to time.

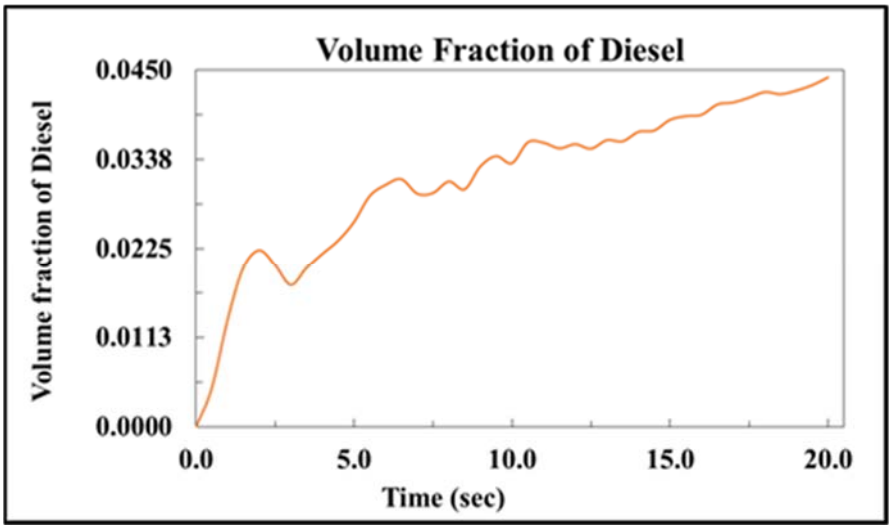

Figure 4.36: Variation of diesel VF with respect to time for h = 0.025 m, d = 0.2 m, ω = 100 rad/s, Fluid pair = Water-Diesel.

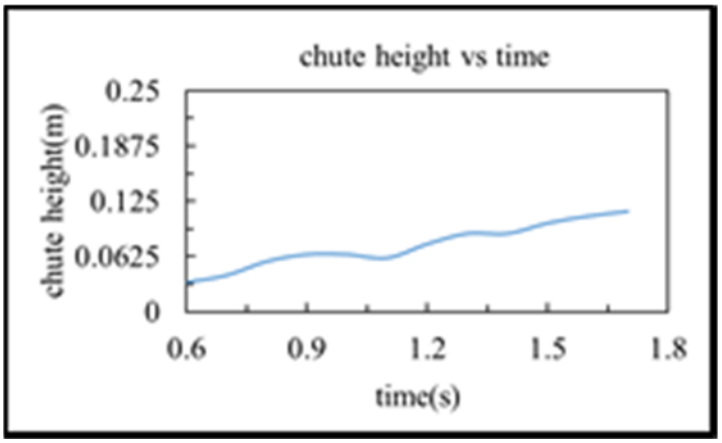

Figure 4.37: Variation of chute height with time for h = 0.025 m, d = 0.2 m, ω = 100 rad/s, Fluid pair = Water-Diesel.

The Figure 4.37 shows the variation of the chute height with respect to time. In this case, the chute height is slowly increasing with time. The Figure 4.38 shows the phase contours at different time instant. In this case very good entrainment is observed as the rotor speed is high, the distance of the rotor from the interface is small and the rotor diameter is sufficiently large.

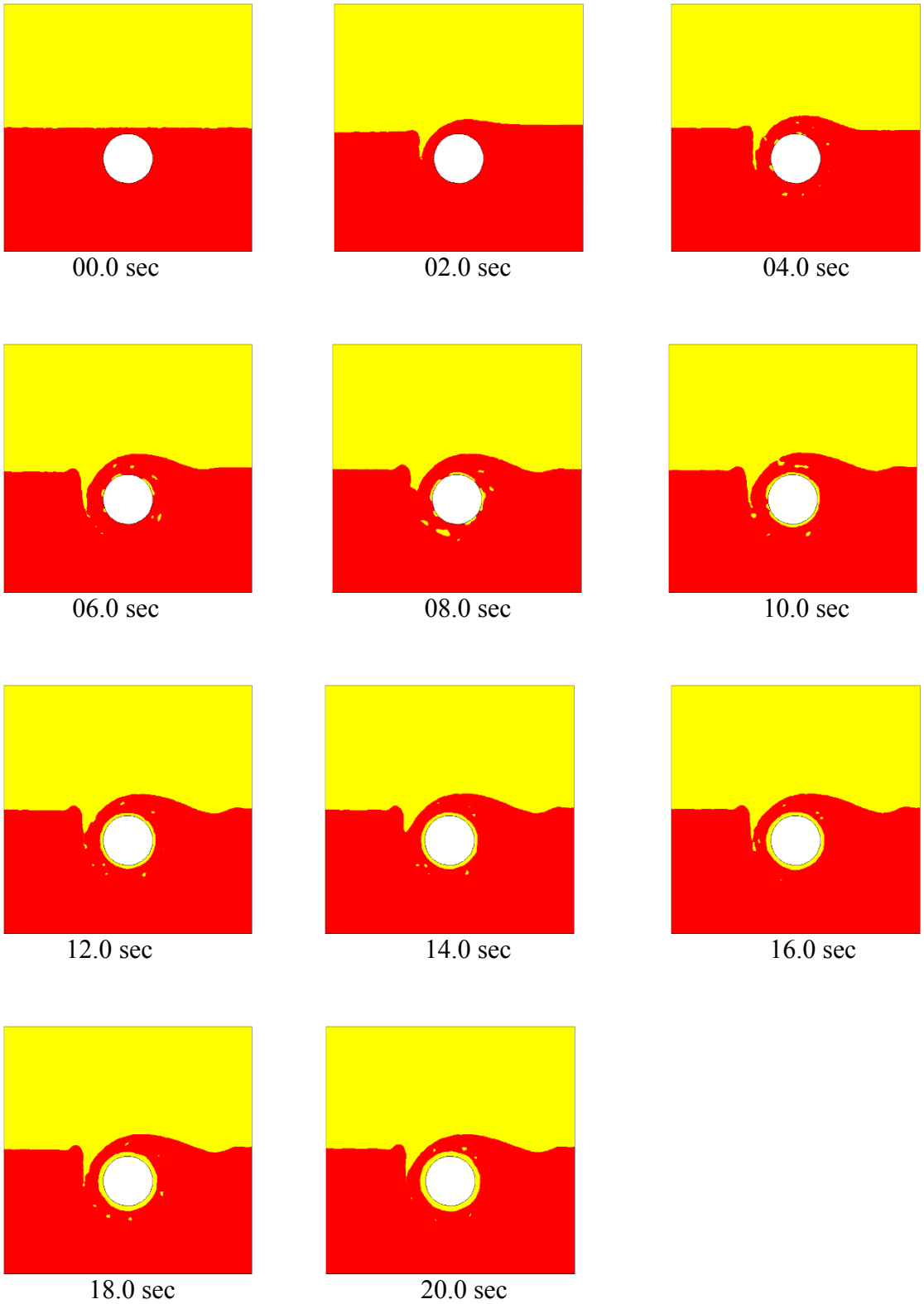

Figure 4.38: The phase contours at different time instants for h = 0.025 m, d = 0.2 m, ω = 100 rad/s, Fluid pair = Water-Diesel.

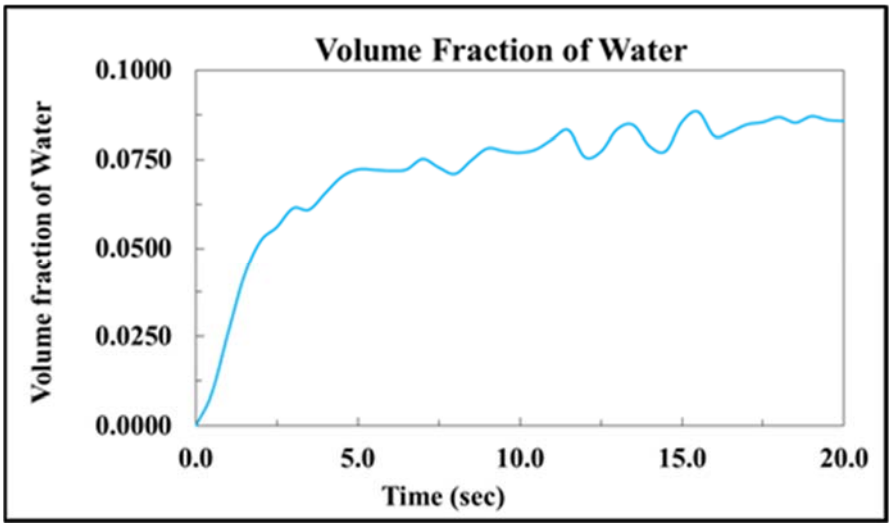

Figure 4.39: Variation of water VF with respect to time for h = 0.025 m, d = 0.2 m, ω = 200 rad/s, Fluid pair = Water-Diesel.

4.1.13 Simulation with h = 0.025 m, d = 0.2 m, ω = 200 rad/s.

For this case, the fluid pair is considered as water-diesel. Here, the rotor diameter (d) is considered as 0.2 m, rotational speed of the rotor (ω) is considered as 200 rad/s, the distance between the interface and the top of the rotor (h) is considered as 0.025 m. The Figure 4.39 shows the Variation of VF of water entrained in to diesel with respect to time. The entrainment is increases with time. In this case the rotor speed is high and the rotor is placed near the interface. Figure 4.40 shows the variation of VF of diesel entrained in water with respect to time. The Figure 4.41 shows the variation of chute height with time. The chute is seen to increase with time .This is because of the high rotor speed.

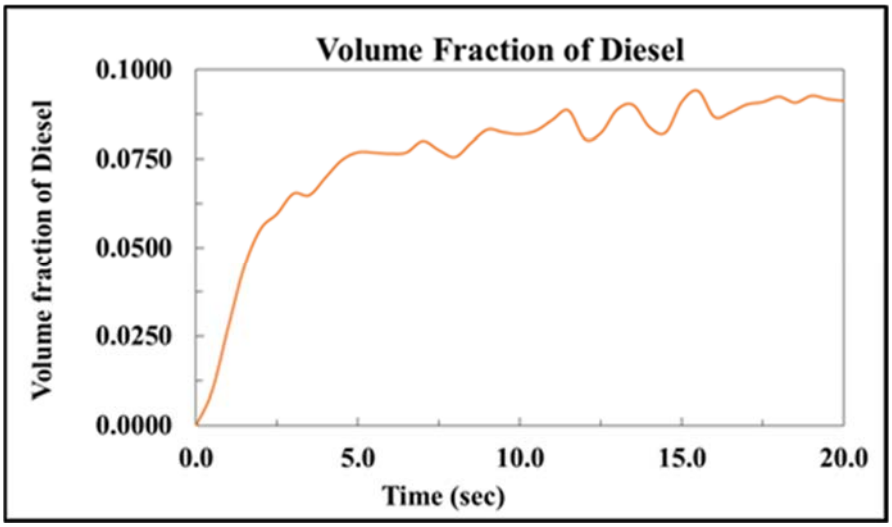

Figure 4.40: Variation of diesel VF with respect to time for h = 0.025 m, d = 0.2 m, ω = 200 rad/s, Fluid pair = Water-Diesel.

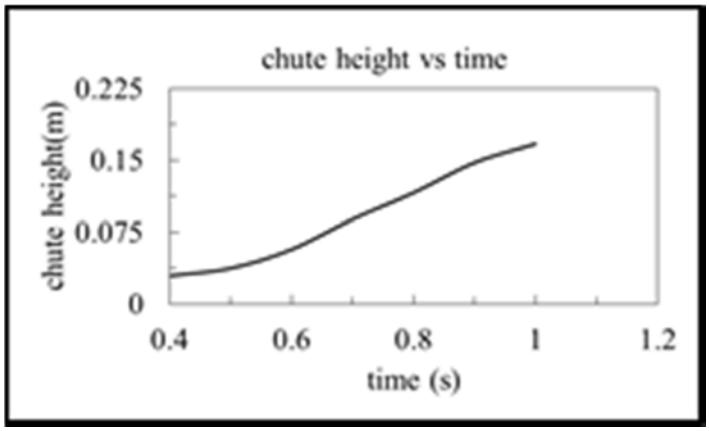

Figure 4.41: Variation of chute height with time for h = 0.025 m, d = 0.2 m, ω = 200 rad/s, Fluid pair = Water-Diesel.

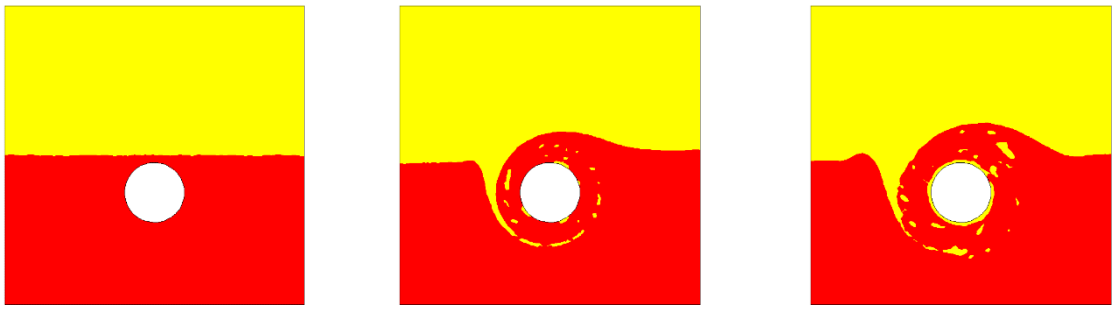

00.0 sec 02.0 sec 04.0 sec

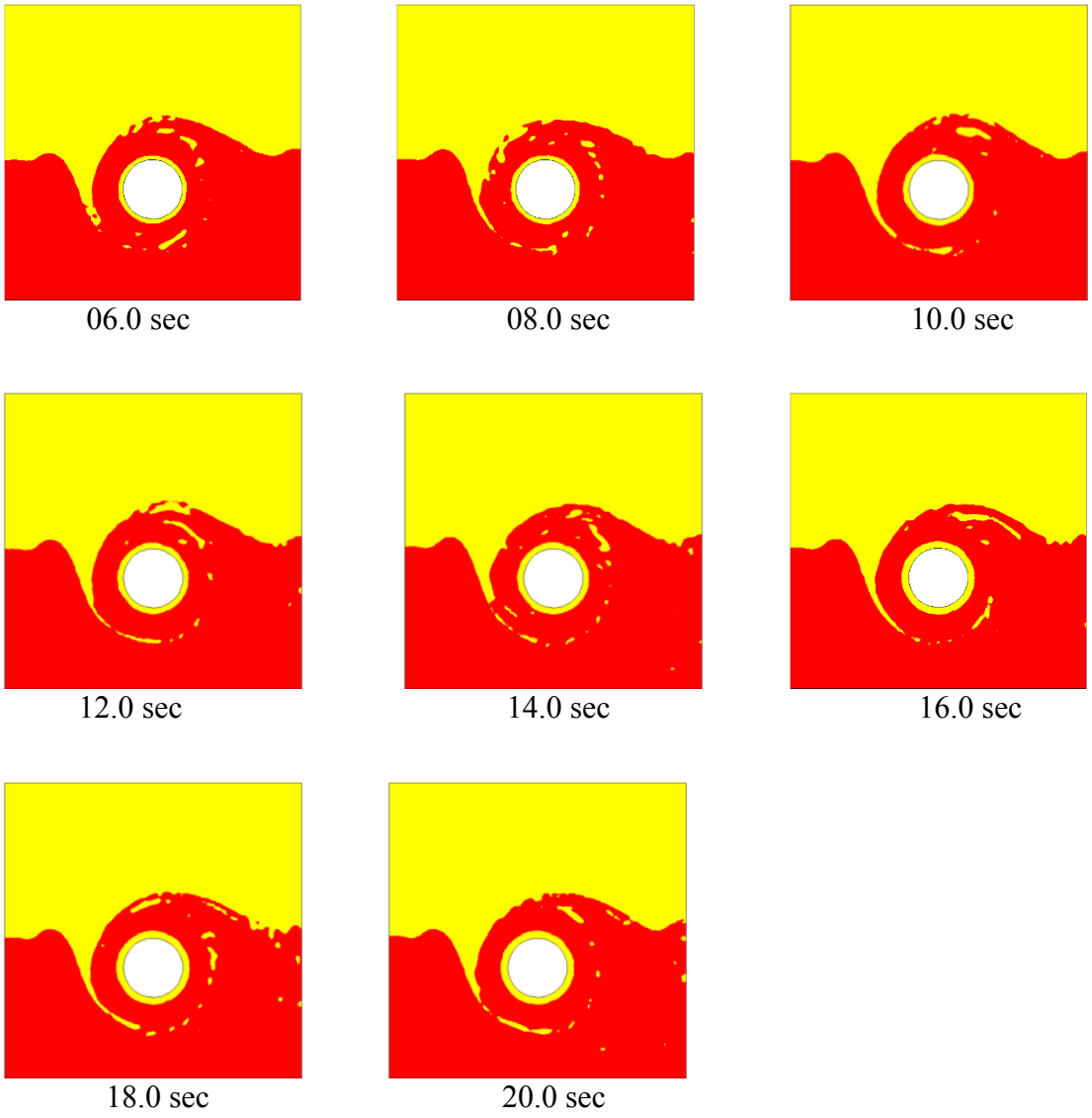

Figure 4.42: The phase contours at different time instants for h = 0.025 m, d = 0.2 m, ω = 200 rad/s, Fluid pair = Water-Diesel.

The Figure 4.42 shows the phase contours at different time instants. As the rotor speed is high and the rotor is placed near to the interface very good entrainment is observed in this case.

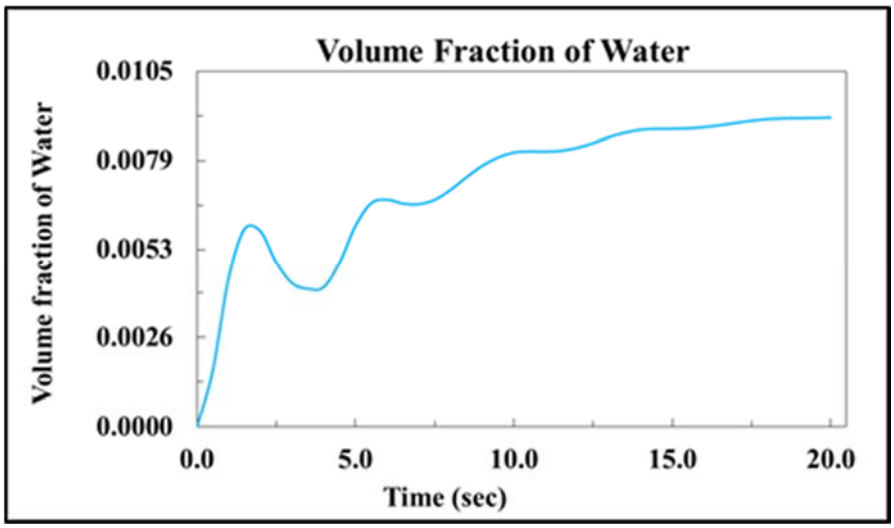

Figure 4.43: Variation of water VF with respect to time for . h = 0.05 m, d = 0.2 m, ω = 50 rad/s, Fluid pair = Water-Diesel.

4.1.14 Simulation with h = 0.05 m, d = 0.2 m, ω = 50 rad/s.

For this case, the fluid pair is considered as water-diesel. Here, the rotor diameter (d) is considered as 0.2 m, rotational speed of the rotor (ω) is considered as 50 rad/s, the distance between the interface and the top of the rotor (h) is considered as 0.05 m. The Figure 4.43 shows the Variation of VF of water entrained in to diesel with respect to time. In this case the volume fraction entrained is increasing with time but the value is small because the rotor speed is not so high. Figure 4.44 shows the variation of VF of diesel entrained in water with respect to time.

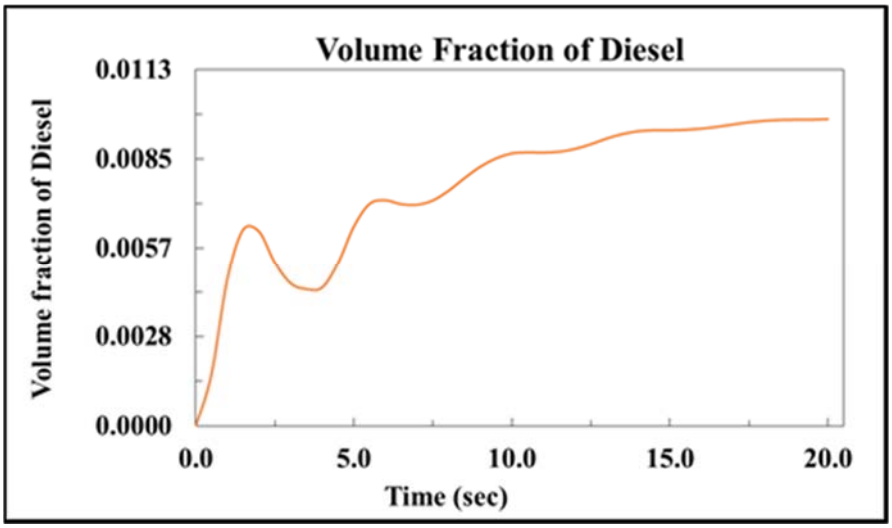

Figure 4.44 : Variation of diesel VF with respect to time for . h = 0.05 m, d = 0.2 m, ω = 50 rad/s, Fluid pair = Water-Diesel.

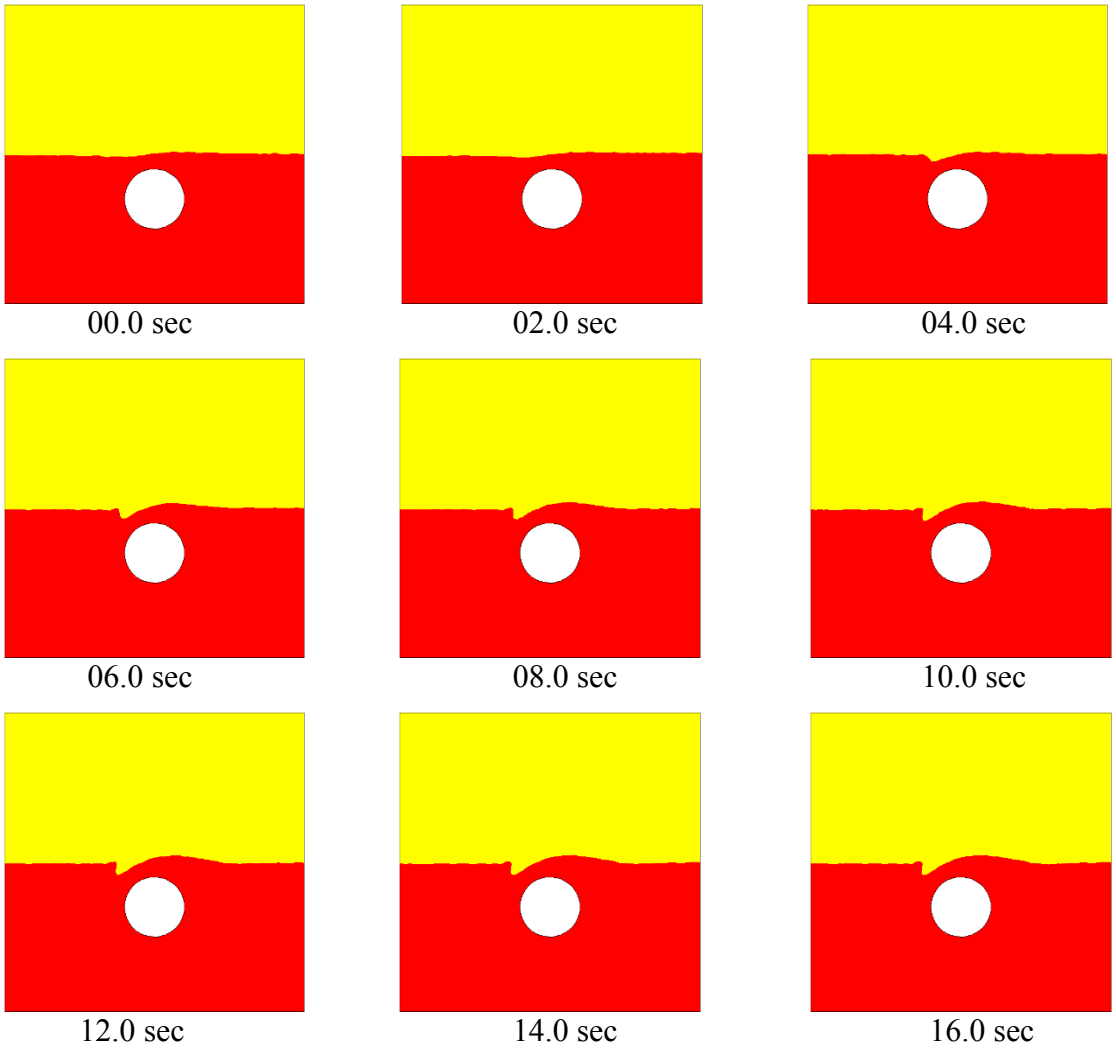

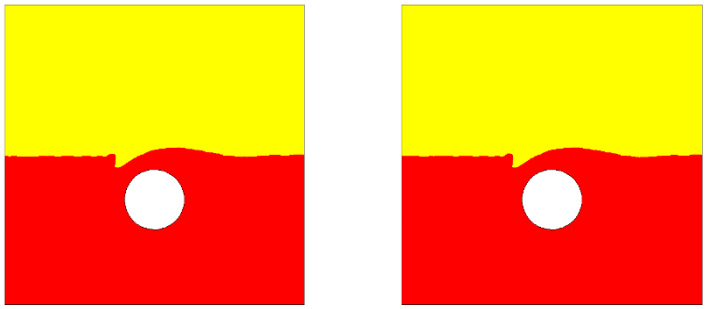

18.0 sec 20.0 sec

Figure 4.45: The phase contours at different time instants for . h = 0.05 m, d = 0.2 m, ω = 50 rad/s, Fluid pair = Water-Diesel

.

The Figure 4.45 shows the phase contours at different time instants. In this case, it is observed that the entrainment rate is less because the rotor speed used is less.

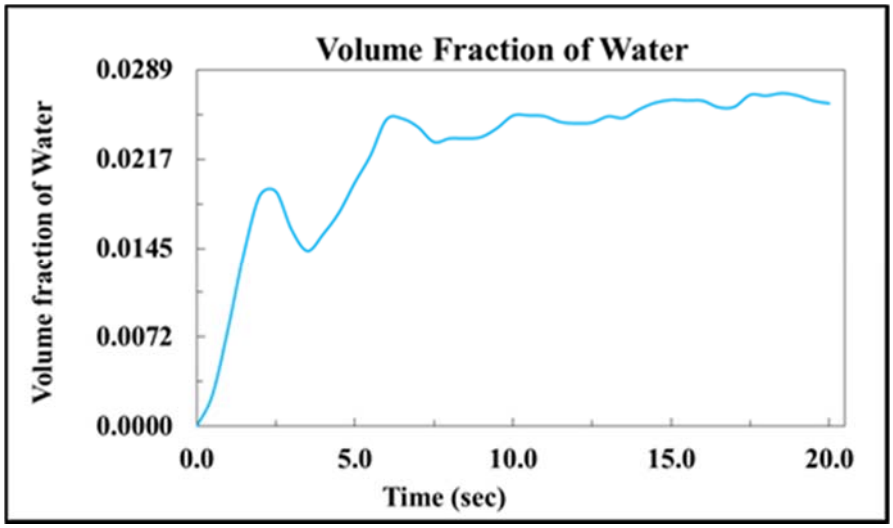

Figure 4.46: Variation of water VF with respect to time for h = 0.05 m, d = 0.2 m, ω = 100 rad/s, Fluid pair = Water-Diesel.

4.1.15 Simulation with h = 0.05 m, d = 0.2 m, ω = 100 rad/s.

For this case, the fluid pair is considered as water-diesel. Here, the rotor diameter (d) is considered as 0.2 m, rotational speed of the rotor (ω) is considered as 100 rad/s, the

distance between the interface and the top of the rotor (h) is considered as 0.05 m. The Figure 4.46 shows the variation of VF of water entrained in to diesel with respect to time. In this case, the volume fraction of the entrained phase is observed to increase with time as the rotor speed is high. Figure 4.47 shows the variation of VF of diesel entrained in water with respect to time.

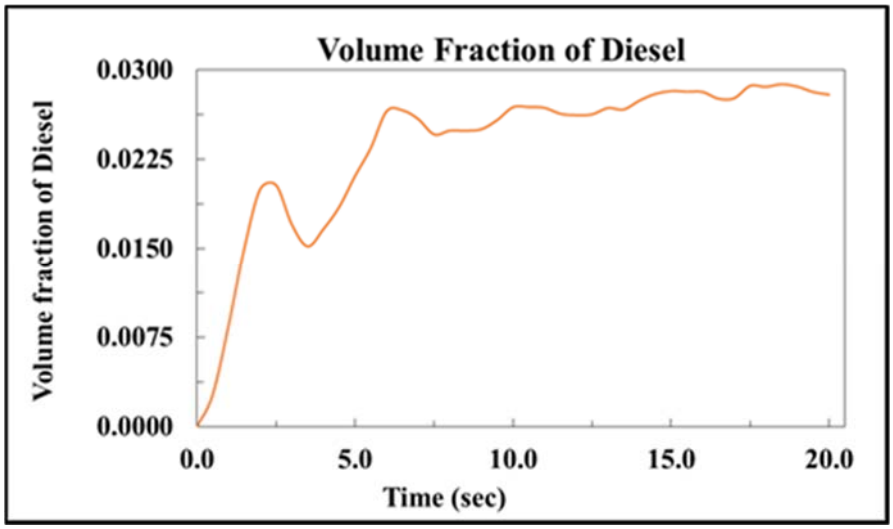

Figure 4.47 : Variation of diesel VF with respect to time for h = 0.05 m, d = 0.2 m, ω = 100 rad/s, Fluid pair = Water-Diesel.

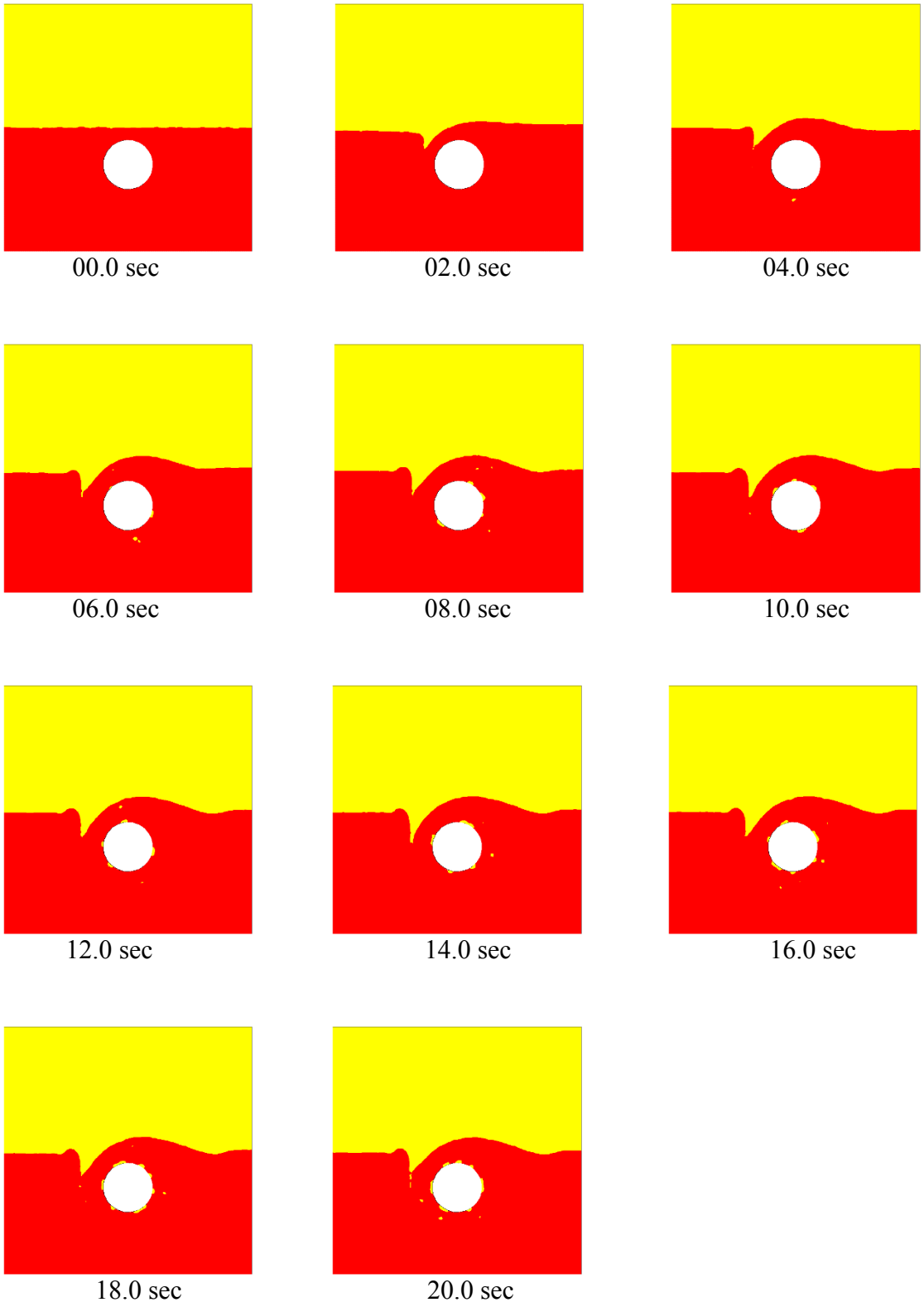

Figure 4.48: The phase contours at different time instants for h = 0.05 m, d = 0.2 m, ω = 100 rad/s, Fluid pair = Water-Diesel.

The Figure 4.48: The phase contours at different time instants in the present case. Here, good entrainment pattern is observed due to the high rotor speed.

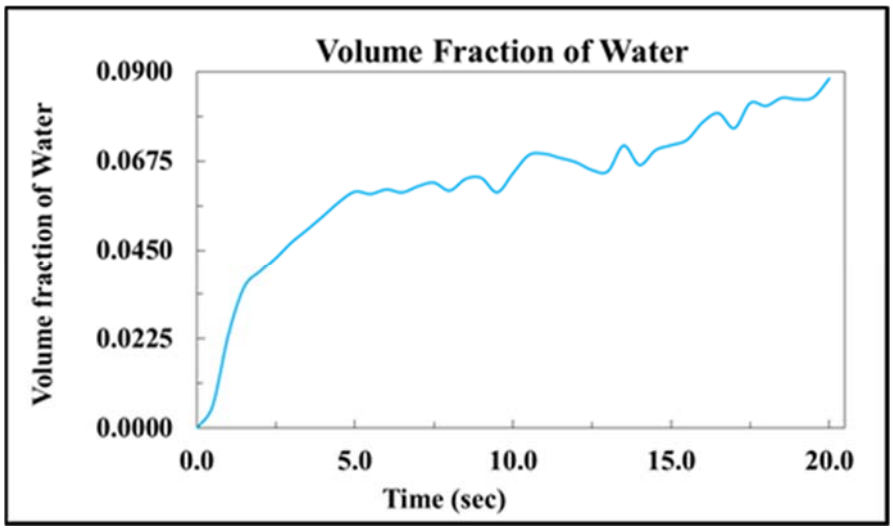

Figure 4.49: Variation of water VF with respect to time for h = 0.05 m, d = 0.2 m, ω = 200 rad/s, Fluid pair = Water-Diesel.

4.1.16 Simulation with h = 0.05 m, d = 0.2 m, ω = 200 rad/s.

For this case, the fluid pair is considered as water-diesel. Here, the rotor diameter (d) is considered as 0.2 m, rotational speed of the rotor (ω) is considered as 200 rad/s, the distance between the interface and the top of the rotor (h) is considered as 0.05 m. The Figure 4.49 shows the variation of VF of water entrained into diesel with respect to time. The volume fraction entrained is increasing with time because the rotor speed is very high in this case. Figure 4.50 shows the variation of VF of diesel entrained in water with respect to time.

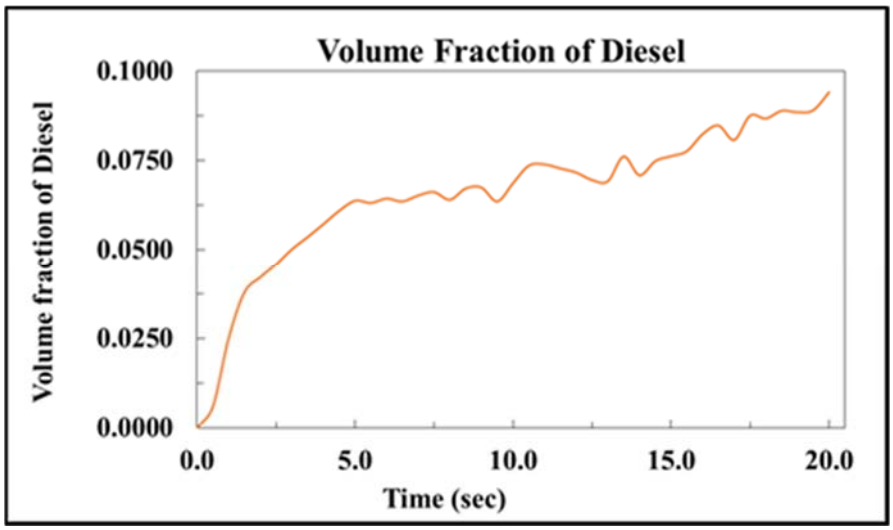

Figure 4.50: Variation of diesel VF with respect to time for h = 0.05 m, d = 0.2 m, ω = 200 rad/s, Fluid pair = Water-Diesel.

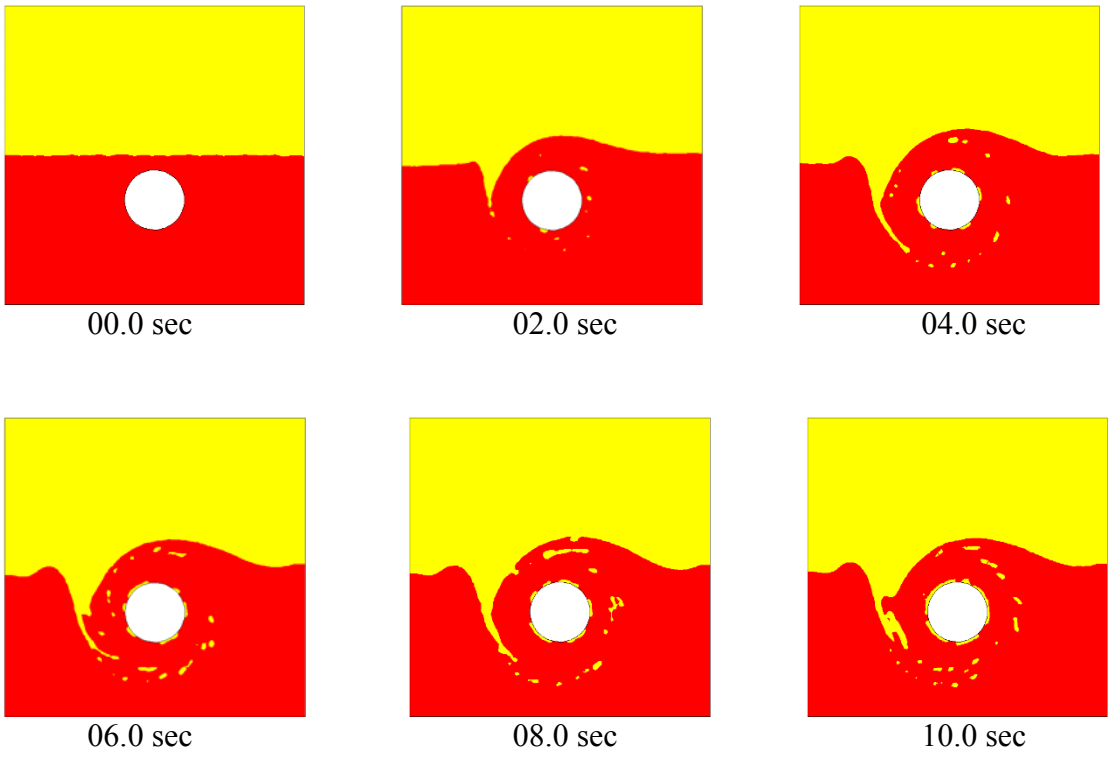

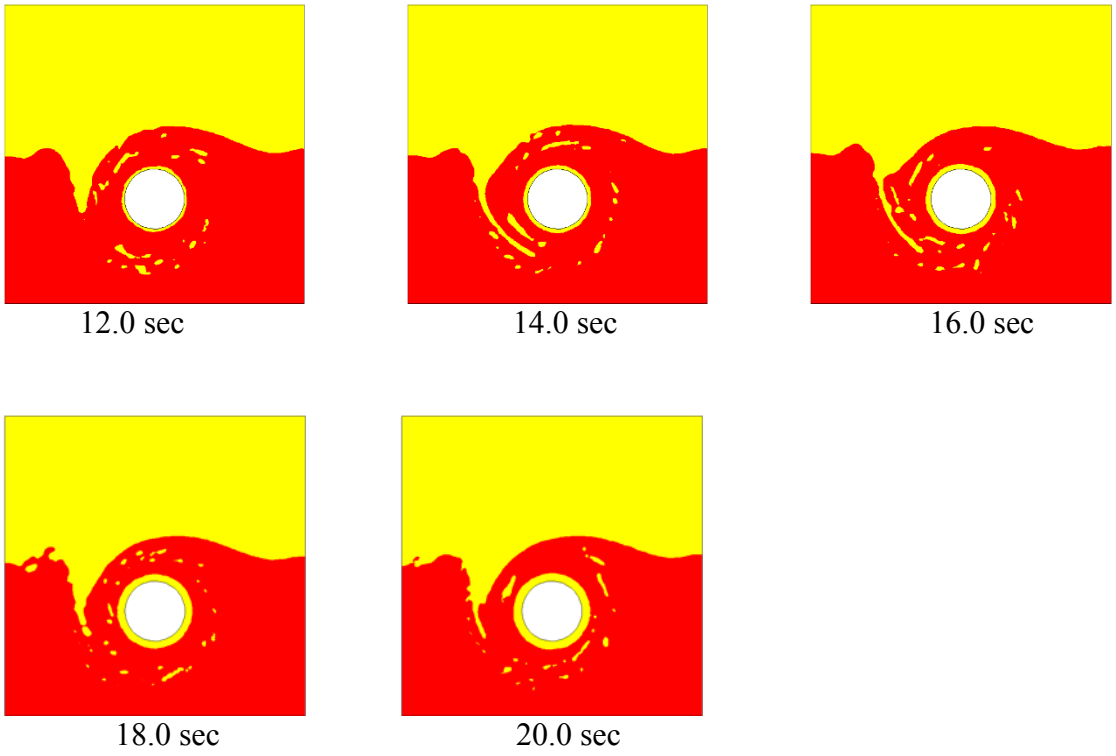

Figure 4.51: The phase contours at different time instants for h = 0.05 m, d = 0.2 m, ω = 200 rad/s, Fluid pair = Water-Diesel.

The Figure 4.51 shows the phase contours at different time instants in the present case. The volume fraction of the entrained fluid is rapidly increases because of high rotor speed and small distance of the rotor from the interface.

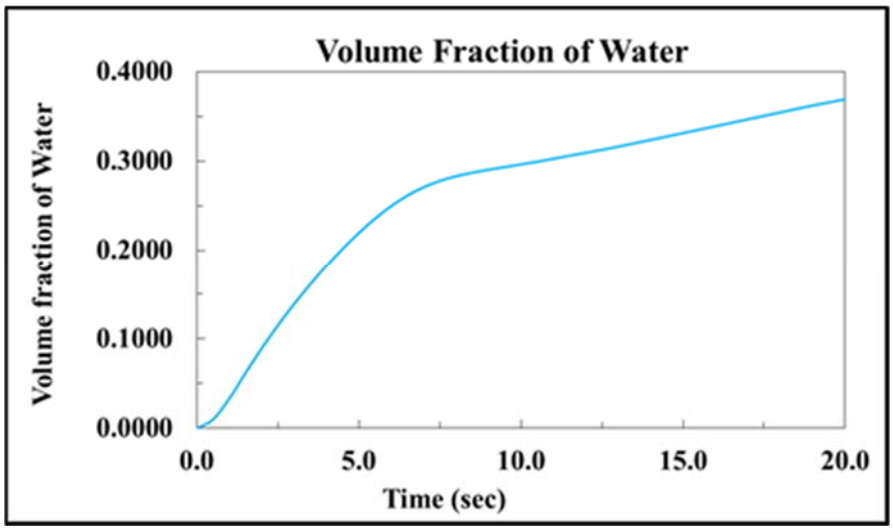

Figure 4.52: Variation of water VF with respect to time for h = 0.025 m, d = 0.2 m, ω = 200 rad/s, Fluid pair = Water-Engine oil.

4.1.17 Simulation with h = 0.025 m, d = 0.2 m, ω = 200 rad/s, Fluid pair = Water-Engine oil.

For this case, the fluid pair is considered as water-engine oil. Here, the rotor diameter (d) is considered as 0.2 m, rotational speed of the rotor (ω) is considered as 200 rad/s, the distance between the interface and the top of the rotor (h) is considered as 0.025 m. The Figure 4.52 shows the variation of VF of water entrained in to diesel with respect to time. In this case instead of water-diesel, water-engine oil has been used as the fluid pair. As a result, very good entrainment is observed as engine oil has a high viscosity than diesel and the interfacial tension is smaller for water-engine oil pair. Figure 4.53 shows the variation of VF of diesel entrained into water with respect to time. Figure 4.54 shows the variation of chute height with respect to time. The chute hieght is continuosly increasing

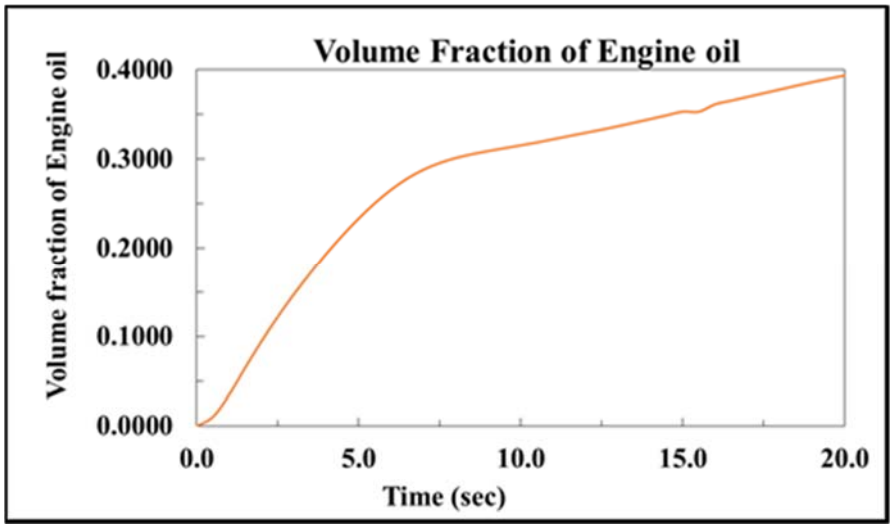

Figure 4.53: Variation of diesel VF with respect to time for h = 0.025 m, d = 0.2 m, ω = 200 rad/s, Fluid pair = Water-Engine oil.

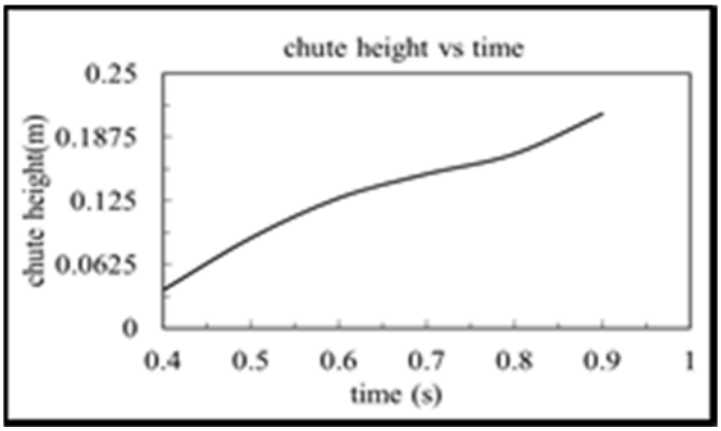

Figure 4.54: variation of chute height with time for h = 0.025 m, d = 0.2 m, ω = 200 rad/s, Fluid pair = Water-Engine oil.

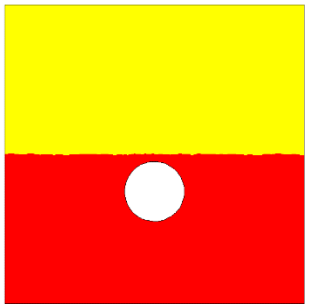
00.0 sec

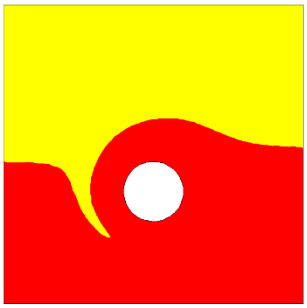
02.0 sec


04.0 sec

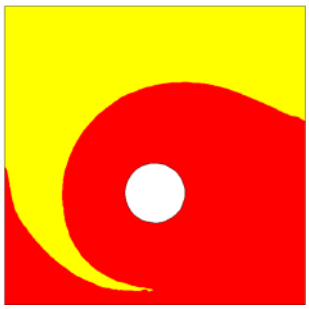
06.0 sec


08.0 sec


10.0 sec


12.0 sec


14.0 sec


16.0 sec

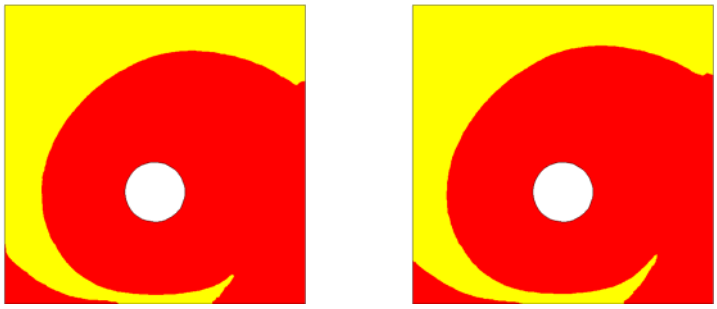

18.0 sec 20.0 sec

Figure 4.55: The phase contours at different time instants for h = 0.025 m, d = 0.2 m, ω = 200 rad/s, Fluid pair = Water-Engine oil.

The Figure 4.55 shows the phase contours of wter and engine oil at different time instants . With water-engine oil fluid pair, more entrainment is observed. Because the engine oil has more viscosity and also due to the effect of interfacial tension.

4.1.18 Effect of parameters on the phenomenon of entrainment

4.1.18.1 Effect of Rotor Speed (ω) on the entrainment phenomena

Figure 4.56 and 4.57 shows respectively the variation of VF of water and diesel entrained with respect to time. In this case the height of the interface from the top of the rotor and the diameter of the rotor has been kept at a constant values of 0.05 m and 0.2 m respectively and the rotor speed is varied. The volume fraction entrained has been plotted for three different rotor speeds of 50 rad/s, 100 rad/s and 200 rad/s and it has been observed that the volume fraction entrained increases with the increase in the rotor speed. As the rotor speed is increased more and more of the lighter phase is being pushed down in to the heavier phase and thereby the volume fraction entrained increases with increase in rotor speed.

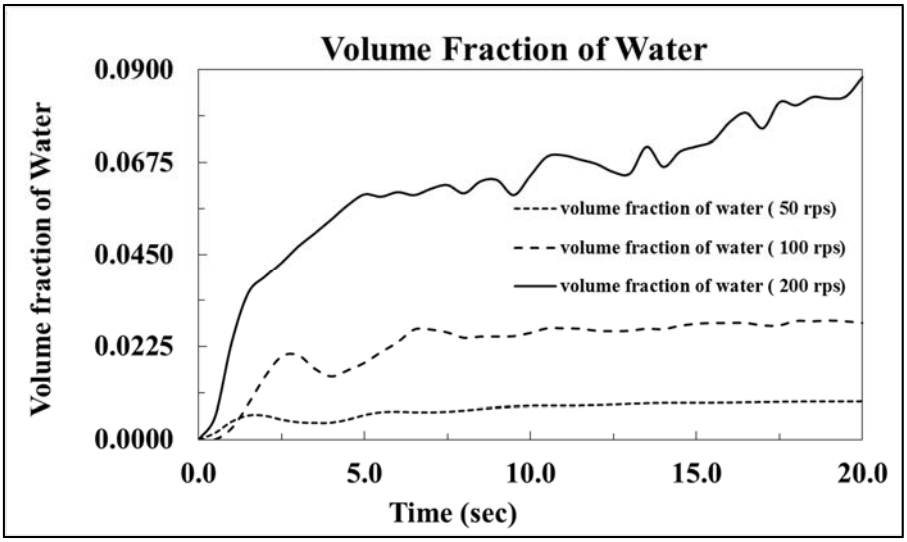

Figure 4.56: Effect of rotor speed on the water entrainment

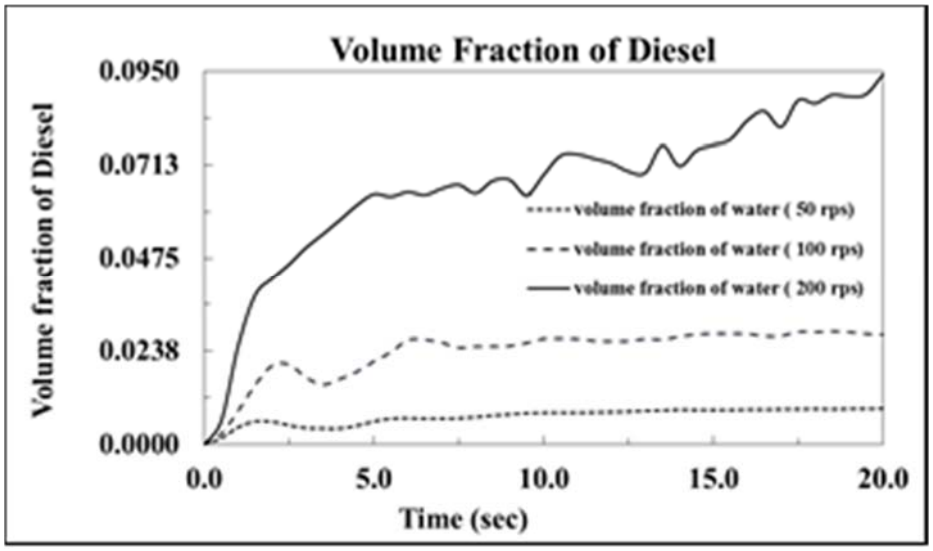

Figure 4.57: Effect of rotor speed on the diesel entrainment.

4.1.18.2 Effect of fluid-pair on entrainment phenomena.

Figure 4.58 and 4.59 shows respectively the variation of VF of water and diesel entrained with respect to time. In this case all the parameters were kept constant and the fluid pair has been varied. The effect of varying the fluid pair has been studied. The fluid pairs used were Water-Diesel and Water-Engine oil. The distance from the rotor top to the interface is 0.025m, the diameter of the rotor is 0.2 m and the rotor speed is

used as 200 rad/s. It has been observed that as the viscosity of fluid increases and the interfacial tension between water and the oil decreases, the entrainment increases.

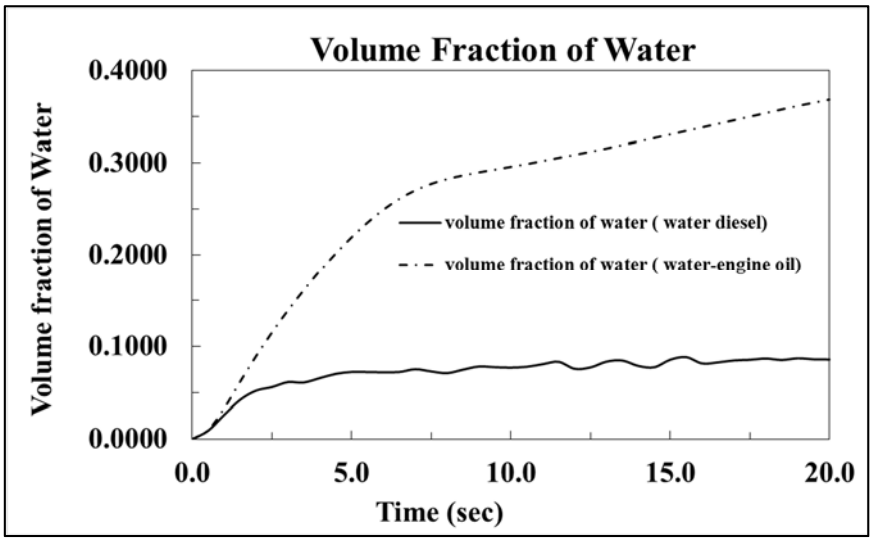

Figure 4.58: Effect of fluid pair on the water entrainment.

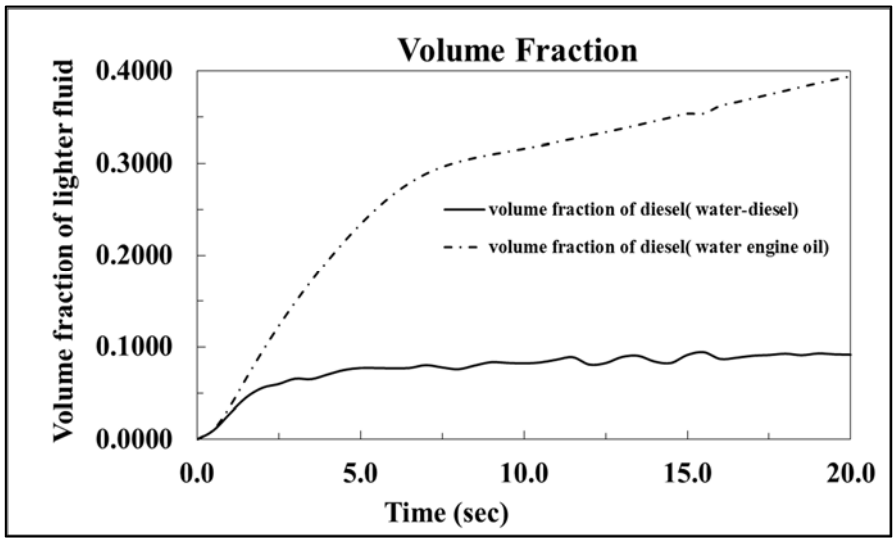

Figure 4.59: Effect of fluid pair on the water entrainment.

4.1.18.3 Effect of distance between rotor top and interface (*h*)

Figure 4.60 and 4.61 shows respectively the variation of VF of water and diesel entrained with respect to time. In this case the distance between the rotor top and the interface has been varied by keeping all the other parameters same. The two heights

(0.05 m and 0.015 m) were considered. The diameter of the rotor is 0.2 m and the rotor speed is considered as 200 rad/s. It has been observed that as the depth increases, the rate of entrainment decreases.

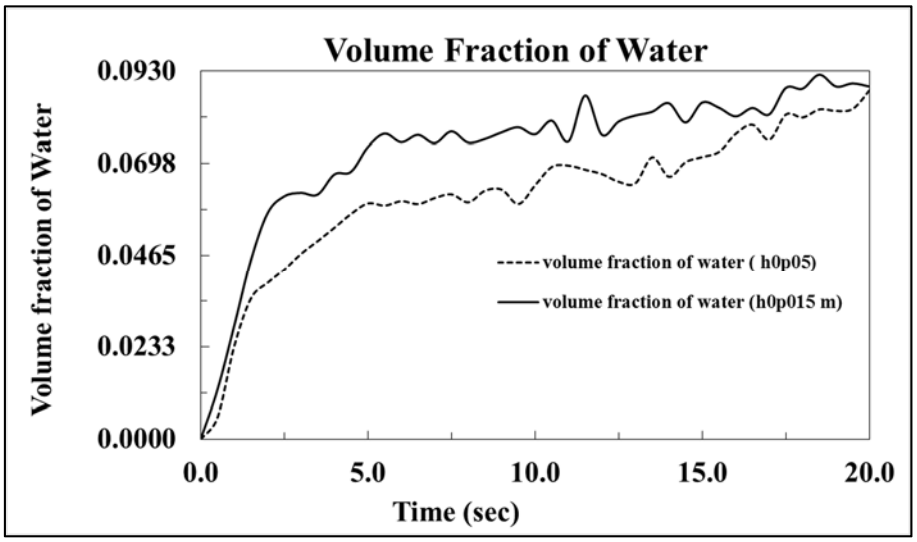

Figure 4.60: Effect of distance between rotor top and interface on the water entrainment.

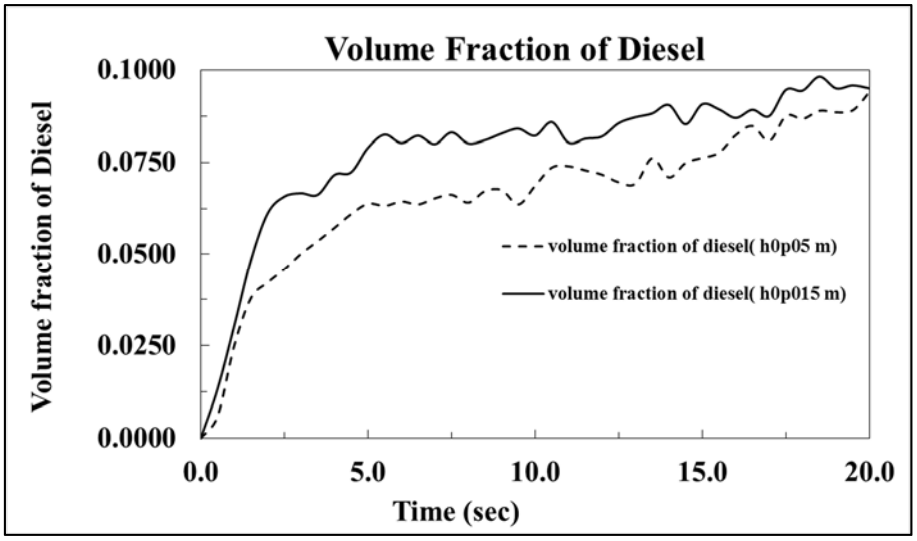

Figure 4.61: Effect of distance between rotor top and interface on the diesel entrainment.

4.1.18.4 Effect of diameter of rotor (d) on entrainment phenomena.

Figure 4.62 and 4.63 shows the variation of VF of water and diesel entrained respectively with respect to time. Here, the fluid pair is considered as water-diesel. The distance from the interface to rotor top is 0.05 m and rotor speed is considered as 10 rad/s. Two diameter are considered (0.1 m and 0.2 m) and it has been observed that as the rotor diameter increases the rate of entrainment also increases.

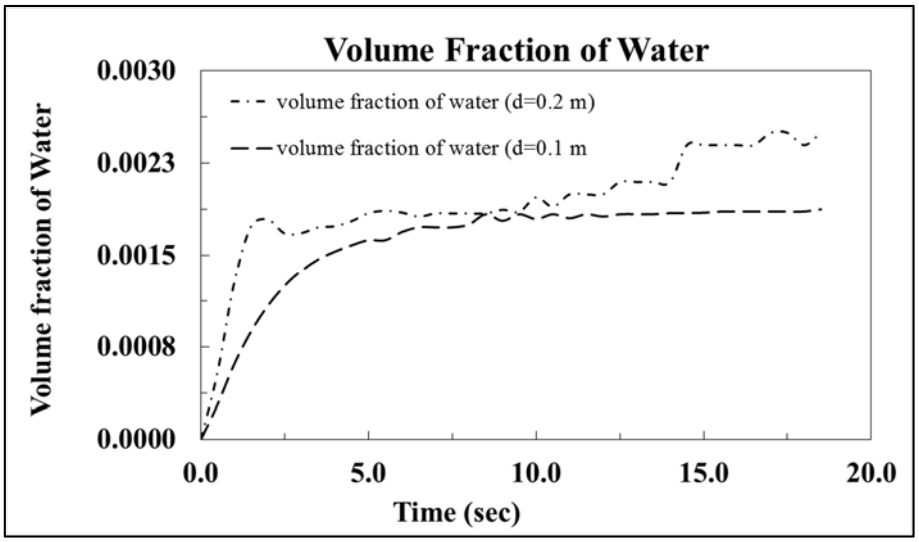

Figure 4.62: Effect of rotor diameter on the water entrainment.

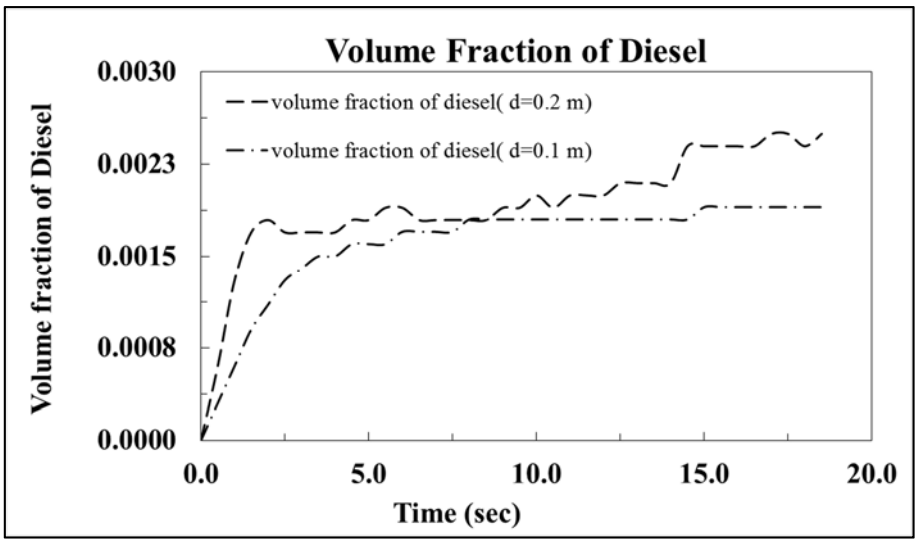

Figure 4.63: Effect of rotor diameter on the diesel entrainment.

4.2 EXPERIMENTAL RESULTS

The experiment is carried out using kerosene-water fluid pair. A cubical tank of side 12 cm is made by perspex sheet and two holes are made on the opposite faces of the tank to insert the rotor. A micro motor is used for running the rotor. The lower half of the tank is filled with water and the upper half of the tank is filled by kerosene. The micro motor is connected to an elemeter for varying the voltage supplied to the micro motor. Two cases are carried out one at 1.5 V supplied to micro motor and the other one at 3.0 V supplied to the micro motor.

4.2.1 Case 1 (1.5 V)

The Figure 4.64 shows the photographs at different time instants during experiment.

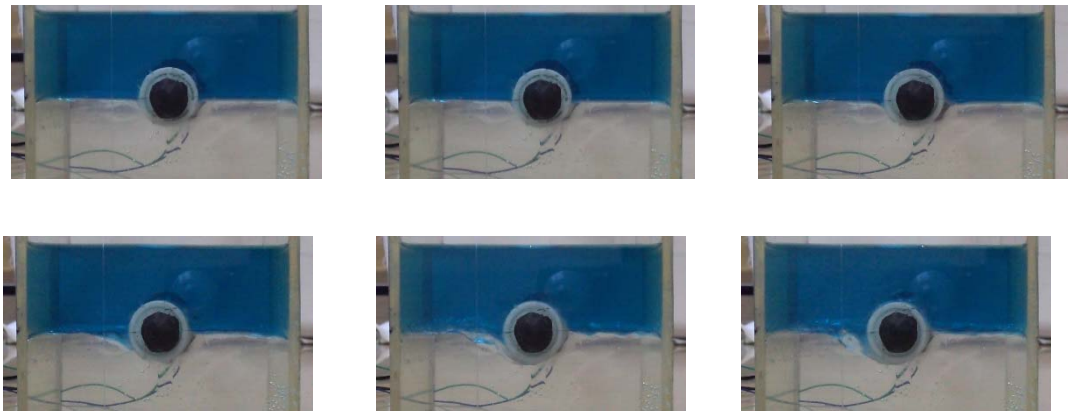

Figure 4.64: Photographs at different time instants during experiment for case1.

4.2.2 Case 2 (3 V)

The Figure 4.65 shows the photographs at different time instants during the experiment.

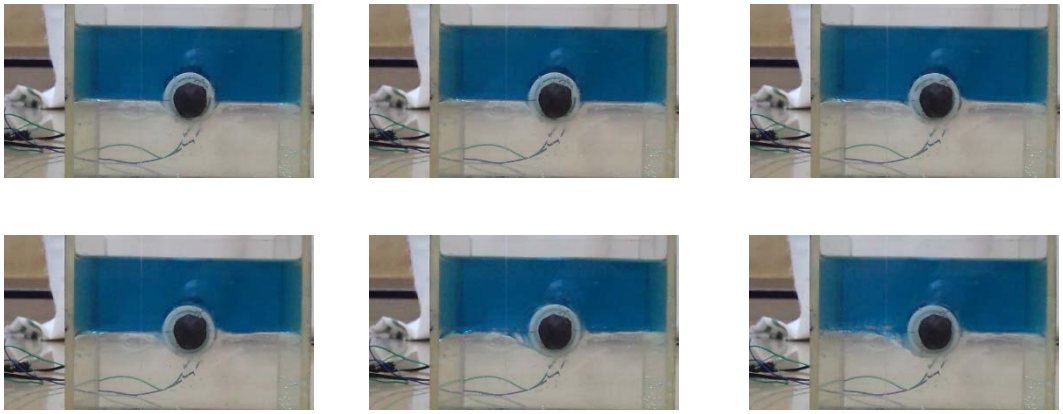

Figure 4.65: Photographs at different time instants during experiment for case 2.

CHAPTER 5:

CONCLUSION & FUTURE SCOPE

5.1 CONCLUSIONS

Study of the entrainment phenomena in a stratified liquid layers by imposing rotary motion using numerical simulation as well as experimental investigation have been carried out. FVM with 2D VOF model has been used to simulate the problem. The different cases were studied by placing a rotor at different locations either in the heavier fluid or in the interfaces. The phenomena has also been studied by varying the rotor diameter and rotor speed. The plot of the VF of the entrained fluid with respect to time and the phase contours at different time instants revealed that the rate of entrainment increases with the decrease in distance of rotor from the interface. Best entrainment is obtained when the rotor is placed at the interface. It has also been observed that the entrainment increases rapidly with the increase in rotor speed. Some important findings extracted from the obtained results are given below.

- For very small rotors and with high distance of the rotor from the interface, entrainment phenomena does not occur.
- The volume fraction of the entrained fluid increases with time.
- With the increase in rotor diameter, the entrainment increases.
- With increase in the speed of the rotor, the entrainment rate is observed to be increasing.
- If the rotor is placed very near to the interface, the entrainment increases.
- The position of the rotor centre at the interface is the most effective position.
- The entrainment pattern varies with the rotor position**.**

5.2 FUTURE WORK

- Entrainment phenomenon in stratified liquid layers by imposing rotary motion has been studied here for two different pair of layers. It can be extended for other liquid pair.
- In the present case, the problem contains only a single stratified liquid layers. In future the same phenomena can be studied by considering more than one stratified layers.
- More than one rotor can be used at different locations in the fluids to study its effect.
- The rotor shape can be changed to study its effect on entrainment.

REFERENCES

FLUENT. (2015) FLUENT user's Guide, Release 15. ANSYS Inc. certified ISO 9001:2008.

Greene, G. A., Chen, J. C., Conlin, M.T., 1991. Bubble induced entrainment between stratified liquid layers. International Journal of Heat and Mass Transfer 34, 149-157.

Kulkarni, A. L., Patwardhan, A W., 2014. CFD modelling of gas entrainment in stirred tank systems. Chemical Engineering Research and Design 92, 1227–1248.

Roy, A. K., Maiti, B., Das, P. K., 2013. Visualisation of air entrainment by a plunging jet. 5th BSME International Conference on Thermal Engineering. Procedia Engineering 56, 468 – 473.

Siavash, N., Robert, R. L., Sergei. A. K., 1986. Entrainment due to turbulent shear flow at the interface of a stably stratified fluid. Tellus 38, 76-87.

Than, P., Preziosi, L., Joseph, D. D., Arney, M., 1988. Measurement of interfacial tension between immiscible liquids with the spinning rod tensiometer. Journal of colloid and interface science 124, 552–559.

Thoroddsen, S. T., Mahadevan, L., 1997. Experimental study of coating flows in a partially-filled horizontally rotating cylinder. Experiments in Fluids 23, 1–13.

Wilkinson, W. L., 1975. Entrainment of air by a solid surface entering a liquid/air interface. Chemical Engineering science 30, 1227-1230.

Wolanski, E. J., Brush, L. M., 1975. Turbulent entrainment across stable density step structures. Tellus 27, 259-268.

Xiaoliang, Q., Afshin, G., Lyes, K., Molki, A., 2013. Experimental characterization of air-entrainment in a plunging jet. Experimental Thermal and Fluid Science 44, 51–61.

Zhaoming, M., Xiaoliang, F., Lei, D., Bo, D., Wenxi, T., Yanhua, Y., Guanghui, S., 2014. Experimental and theoretical investigation of liquid entrainment through small-scaled ADS-4 in AP1000. Experimental Thermal and Fluid Science 57, 177–187.